

Predicting the Thermodynamic Properties and Dielectric Behavior of Electrolyte Solutions Using the SAFT-VR+DE Equation of State

Gaurav Das, Stepan Hlushak, and M. Carolina dos Ramos

Dept. of Chemical and Biomolecular Engineering, Vanderbilt University, Nashville, TN 37235

Clare McCabe

Dept. of Chemical and Biomolecular Engineering, Vanderbilt University, Nashville, TN 37235

Dept. of Chemistry, Vanderbilt University, Nashville, TN 37235

DOI 10.1002/aic.14909

Published online August 7, 2015 in Wiley Online Library (wileyonlinelibrary.com)

We extend the SAFT-VR+DE equation of state to describe 19 aqueous electrolyte solutions with both a fully dissociated and a partially dissociated model. The approach is found to predict thermodynamic properties such as the osmotic coefficient, water activity coefficient, and solution density, across different salt concentrations at room temperature and pressure in good agreement with experiment using only one or two fitted parameters. At higher temperatures and pressures, without any additional fitting, the theory is found to be in qualitative agreement with experimental mean ionic activities and osmotic coefficients. The behavior of the dielectric constant as a function of salt concentration is also reported for the first time using a statistical associating fluid theory (SAFT)-based equation of state. At high salt concentrations, the stronger electrostatic interactions between the ionic species due to the dielectric decrement, is captured through the inclusion of ion association. © 2015 American Institute of Chemical Engineers AIChE J, 61: 3053–3072, 2015
Keywords: aqueous solutions, liquids, water activity, salt, thermodynamics/statistical, mechanics

Introduction

From natural biological systems to industrial chemical processes such as osmosis and reverse osmosis, fertilizer production, water purification, geochemistry, electrochemistry, and enhanced oil recovery, the ubiquitous presence of electrolytes has made the thermodynamic study of these fluids an active area of research both experimentally and theoretically.^{1–5} These are, however, challenging fluids to study as the presence of long-range Coulombic interactions between the ionic species makes electrolyte solutions highly nonideal.⁶ In any theoretical investigation of electrolyte solutions, describing the complex nature of the electrostatic interactions present between the ionic species and the ions and the aqueous solution is key.^{7,8}

One approach to address the thermodynamics of electrolyte solutions is through the use of an implicit solvent model, that approximates the dipolar water solvent by a constant dielectric continuum, which presents a simplistic view of the complexity of the interactions involved in these systems. Often, Debye–Hückel (DH) theory, which considers point charges in a dielectric medium, is used to represent the electrostatic behavior in equation of state used to model electrolyte solutions. Several semiempirical equation of state and modified versions

of activity coefficient models rooted in DH theory have also been proposed, such as the Pitzer equations^{7,9,10} and the electrolyte nonrandom two-liquid model,¹¹ among others.^{11–21} This kind of implicit treatment of the solvent is also known as a McMillan–Mayer (MM) level²² model and is more generally referred to as a primitive model.²³ Implicit treatment of the solvent, although widely used to describe thermophysical properties of electrolyte solutions, has limitations in terms of capturing the effects of the solvent-ion interactions as they are solely described through the solvent dielectric constant.

A step toward a more accurate description of ionic species in dipolar solvents is introduced via Born–Oppenheimer (BO) models,²² in which the solvent species appear explicitly in the model and are also referred to as non-primitive models. In the simplest case, a BO level model can be conceptualized as a mixture of charged hard spheres in a solvent of hard spherical molecules with a point dipole embedded in the center. For further complex cases, higher order multipole moments or discrete charges at a specified position within the ion can be included.

Analytical expressions to calculate the free energy and thermodynamic properties have been derived for both MM and BO models. Broadly, two kinds of statistical mechanics-based approaches are used, perturbation theory and integral equation theory. Stell and Lebowitz²⁴ were the first to derive a perturbation term for the Helmholtz free energy for the ion-ion interaction from DH theory. Henderson²⁵ later proposed a restricted perturbation theory (i.e., an equimolar mixture of equal-

Correspondence concerning this article should be addressed to C. McCabe at c.mccabe@vanderbilt.edu.

diameter hard spheres are assumed in a dielectric continuum) in which the ion-ion interaction is treated as a perturbation term. In a subsequent effort, Henderson²⁶ extended the approach for ion-dipole interactions and Jin and Donohue^{27–29} further refined the theory by combining, the perturbed-anisotropic-chain theory (expressions for short-range interactions) with Henderson's primitive model expressions for the ion-ion interactions. With integral equation theory, generally the hypernetted chain (HNC)³⁰ or the mean spherical approximation (MSA) are used to solve the relation between the direct correlation function and the pair correlation function given by the Ornstein–Zernike (OZ) equation. Although the HNC approximation is more accurate, it is mathematically more complex and unlike the MSA, does not provide analytical solutions to the OZ equation. The MSA approach, introduced by Percus, Yevick, and Lebowitz^{31,32} to solve the OZ equation, has been analytically solved for a wide range of important model systems such as the hard-sphere,³³ Yukawa,³⁴ and dipolar hard-sphere fluids,³⁵ electro-neutral mixtures of hard charges,³³ and plasma³⁶ (charges in neutralizing background), mixtures of hard dipoles^{37,38} and hard ions with dipoles.^{39–41} The MSA was first applied in the primitive model by Waisman and Lebowitz³³ and Blum⁴² and analytical expressions for the thermodynamic properties of both the restricted and unrestricted primitive MSA models were obtained. In the primitive model expressions for the MSA, the effect of the volume of the ions is taken into account explicitly and when the diameters of the ions is reduced to zero the MSA expressions reduce to point charges and the DH equation. Later Blum⁴³ and Adelman and Deutch³⁸ developed analytic solutions for the non-primitive MSA (NPMSA) by explicitly including the effect of the solvent, yielding expressions for the thermodynamic properties of a mixture of equal sized ions and dipolar hard spheres. In subsequent work, Blum and Wei⁴⁰ extended the solutions to a system of arbitrary sizes of charged and dipolar hard spheres. The solution of the NPMSA includes three types of interactions: ion-ion, ion-dipole, and dipole-dipole. Explicit forms for the ion-ion, ion-dipole, and dipole-dipole pair distribution functions was later developed by Hoye and Stell⁴⁴ using the approach proposed by Blum and Wei.⁴⁰ For a comprehensive review of theories developed for aqueous electrolyte fluids, the reader is directed to the excellent reviews of Loehe and Donohue,⁸ Anderko et al.,⁵ and McCabe and Galindo.⁴⁵ Since the focus of this work is on the further development and application of the statistical associating fluid theory (SAFT)-based approach of Zhao et al.⁴⁶ to experimental electrolyte systems, we will limit the remaining discussion to SAFT-based approaches to describe electrolyte solutions.

SAFT,^{47–49} based upon Wertheim's first-order thermodynamic perturbation theory,^{50–53} is a statistical mechanics-based equation of state that in various forms has been used to describe the phase behavior of a wide range of industrially important complex fluid systems.^{45,54–56} Among the many variations of SAFT are several approaches to describe electrolyte systems.^{46,57–59} The study of electrolytes with SAFT-derived equations of state can be broadly divided into two categories: those based on the primitive and non-primitive models. In one of the first developments Galindo et al.⁵⁷ applied a modified version of SAFT, termed SAFT-VRE, to describe strong-real electrolyte solutions. The MSA was used at the level of the restrictive primitive model (RPM) to account for the charged interactions, while the water-water and ion-water attractive interactions were described via square-well (SW) dispersive

interactions. The results from the SAFT-VRE approach using ion-specific (rather than salt-specific) parameters were found to be in good agreement with experimental vapor pressure and solution density data for electrolytes up to concentrations of 10 mol/L between 273 and 373 K. However, although a wide range of temperatures were studied, the ability of the theory to describe more sensitive thermodynamic properties such as the osmotic coefficient and mean ionic activity coefficient were not considered and hydration effects were not discussed. In more recent work, Schreckenber et al.,⁶⁰ proposed an improved formulation of SAFT-VRE that incorporates a Born term to describe the contribution due to the solvation of ions at infinite dilution. While this improves the theoretical treatment of solvation effects by partially addressing the poor solvation behavior that results from using a primitive model, ion-polar and polar-polar interactions are still not explicitly described. The implicit solvent within the primitive model framework of SAFT-VRE was represented through an empirical solution dielectric constant model, following the work of Uematsu and Franck,⁶¹ which takes into account the temperature, density, and composition of the solvent and in turn makes the dielectric constant a differentiable variable. The electrolytes were described using a fully dissociated model and ion-specific interaction parameters, with the effective ionic diameter, ion-solvent, and ion-ion dispersive energy parameters fitted to vapor pressure, solution density, and mean ionic activity coefficient data for 15 different alkali halide salts at temperatures below 523 K. The cross ion-ion dispersive interaction energy was estimated using a procedure proposed by Hudson and McCoubrey.⁶² Although the theory was shown to provide a good representation of correlated properties (<5% in most cases) and predicted properties such as osmotic coefficients (<5% in most cases) and freezing temperature depression (for NaCl, LiCl) at 1 bar pressure, an accurate quantitative prediction of the free energy of solvation (average error ~35%) was not possible. The study was subsequently extended to predict the vapor pressures and solution densities of multisalt systems over a range of temperature (298.12–397.97 K) and pressure (0.92–68.42 MPa) without fitting any additional parameters. Mixed solvent electrolytes (methanol/*n*-butanol and water + salt systems) were also studied with the alcohol-ion unlike dispersion energy parameter obtained by fitting to experimental water + alkanol + salt VLE/LLE data and good agreement with the experimental results were obtained. In related work, Tan et al.⁵⁸ combined the RPM with the SAFT1 (a variant of SAFT-VR) equation of state to treat electrolyte solutions. Ions were described as hard charged spheres and hence only water-ion and water-water dispersive interactions were considered. To parameterize the model, a hydrated ion diameter (salt-specific property) along with ion-specific volumes and ion-water dispersion (hydration) energies, were obtained by fitting to experimental data for the mean ionic activity coefficient and salt densities for individual salt solutions. To accurately correlate the experimental data, all model parameters and the water dielectric constant, which was determined from an empirical equation, were made temperature dependent. The approach was then used to predict the osmotic coefficient and vapor pressures for Cl⁻, Br⁻, I⁻ salts of Na⁺, K⁺, and Li⁺ at 298.15–373.15 K with very low deviations (<1% for most cases) from experimental data. Ji et al.^{63,64} later extended the approach to study mixed salt solutions and introduced a mixing rule for the hydrated ion diameter with a binary adjustable parameter for each pair of salts studied. The binary adjustable

parameters (referred to as l_{ij} in their work) were obtained from fitting to the osmotic coefficient for ternary salt solutions (i.e., two salts + water) and then used to predict the solution densities and osmotic coefficient of quaternary solutions (i.e., three different salts + water). One should note that the use of an additional adjustable parameter (i.e., l_{ij} along with the ionic volume and ion-water dispersion energy) further reduces the predictive ability of the theory. Behzadi et al.⁵⁹ also used a version of the SAFT-VR equation of state, but with a Yukawa potential and the nonrestricted MSA as extended by Blum^{42,65} to study the vapor pressure, solution densities, and activity coefficients of electrolyte solutions. Long-range Coulombic interactions between ionic species were taken into account using the nonrestricted MSA, while solvent-solvent and solvent-ion dispersion interactions were described through the Yukawa potential. Twenty-three salts in seven different solvents (water and alcohols) were studied using three different parameterization schemes: ion-specific, cation-specific, and salt-specific. In each case, the dispersion interaction was optimized by fitting to experimental vapor pressures and liquid volumes while the cross-interaction range parameter was fixed at 1.2. The ionic radii were taken to be the Pauling radii or thermochemical radii whichever was available for a specific ion. To test the thermodynamics of the model, the mean ionic activity of LiCl and NaCl were predicted and the salt-specific parameters were found to give more accurate predictions compared to the ion-specific and cation-specific ones. Also, in this work the Yukawa-based approach was compared with the more commonly used SW potential and the Yukawa model found to give slightly better results.

Focusing on DH approaches, Cameretti et al.⁶⁶ extended the perturbed chain SAFT (PC-SAFT) equation to electrolyte systems by taking into account the electrostatic interactions in ionic solutions using a simple DH term. The resulting ePC-SAFT equation of state was found to be able to accurately correlate and predict the vapor pressures of single- and mixed-salt (NaCl-KBr, NaBr-KCl) solution densities up to high salt concentrations ($>6 m$ for some salts, including 12.7 m for LiCl and 13.8 m LiBr). Only two salt-specific parameters, the hydrated ion diameter and water-ion dispersion energy (for both cations and anions), were required and obtained by fitting to experimental vapor pressure and density data. In an extension of this work, Held et al.^{67,68} subsequently studied both VLE and the mean ionic activity coefficient of both weak and strong aqueous electrolyte solutions. The previously developed ion-specific diameter and dispersive energy parameters of Cameretti et al., which were obtained by only fitting to vapor pressure and solution densities, were found to be inaccurate in describing the mean ionic activity coefficient and so ion-specific diameters and dispersive energies were determined by fitting to the mean ionic activity coefficient and salt solution density data. The water model was also revised to include a temperature-dependent diameter. With these modifications, the ePC-SAFT equation was found to provide an accurate description of the thermodynamics of 115 aqueous electrolyte solutions at 298.15 K. Subsequently, the equation of state was successfully extended to mixed solvent electrolyte systems by representing the solvent with an effective dielectric constant calculated from empirical equations dependent upon temperature and the mixture solvent composition.⁶⁹ With this primitive-model-based approach, solution densities and mean ionic activities of KCl, NaBr, NaCl, NaI, LiCl in ethanol + water, methanol + water, and methanol + ethanol + water

mixed solvents were studied across different weight fractions of solvent and found to represent the experimental data accurately.

In an alternative approach, Liu et al.⁷⁰ combined the original SAFT approach (in which the dispersion term is given by the expression of Cotterman et al.⁷¹) with the primitive model expressions obtained from the MSA and Henderson–Blum–Tani²⁶ perturbation theory expansion for the ion-dipole and dipole-dipole terms to study aqueous single salt and mixed salt systems at 298.15 K. Salts were modeled as LJ spheres using the Pauling diameter for the anion and the cation diameter as an adjustable parameter that was obtained by correlating experimental mean ionic activity coefficient data. The Mavroyannis–Stephen equation,⁷² which calculates dispersion energy for individual ions based on the ionic radii, number of electrons, and polarizability, was used to obtain the dispersive interaction parameters for the ions. Thirty single and thirteen-mixed salt electrolyte systems were studied with good accuracy (% average absolute deviation (AAD) for the mean ionic activity coefficient and density was $<3\%$ for concentrations up to 6 m). In subsequent work, Liu et al.⁷³ modified the approach to include the low-density expansion⁷⁴ of the solution of the primitive MSA to describe ion-dipole interactions. We note that although the theory is described as a non-primitive approach, when the solvent volume is neglected, as is done by the authors, the expression for the ion-solvent term reduces to the Born expression in the primitive model. The ions were again described as charged LJ spheres with the Pauling ionic radii used for the ion-ion, dispersive and associative SAFT terms and an effective average ion radii (representing a Born type ionic radii) used for the ion-solvent term. The ion dispersive energy parameters were again obtained using the Mavroyannis–Stephen equation. To effectively capture the ion-solvent interactions, a SAFT association term was considered between the ions and solvent with several association sites^{7–12} being placed on the ions. The effective average ion radii and SAFT association energy between the ions and solvent was obtained by fitting to experimental mean ionic activity coefficient data. Both salt dependent and salt independent parameters were investigated, with salt-dependent parameters found to provide lower deviations. Furthermore, if the anion-solvent association was removed from the model, and only cation-solvent association considered, there was little to no impact observed on the correlated results. Using the fitted parameters, the density, osmotic coefficient, and water activity were then predicted for 15 different aqueous electrolyte salts with $<2\%$ AADs. The predicted water activity and osmotic coefficient was compared with those from Jin and Donohue²⁷, Myers et al.,⁷⁵ and Fürst et al.⁷⁶ and the proposed approach found to be superior in terms of the % AADs with experiment.

More recently, Rozmus et al.⁷⁷ developed the ePPC-SAFT equation of state by combining the polar perturbed chain (PPC)-SAFT equation of state with the MSA for a primitive model of electrolyte solutions. Association sites between the ions and solvent were considered to describe the ion-solvent interactions and a Born term was included in addition to the MSA term for electrostatics to describe the change in the dielectric constant resulting from the solvation of the ionic species. The dielectric constant of the water solvent was made temperature and solution density dependent using an empirical equation proposed by Schimdt and Grigull.⁷⁸ Ion-specific diameters and association energies were obtained by fitting to mean ionic activity coefficient and apparent molar volume

data for 19 alkali-halide aqueous solutions. The performance of the approach was then tested through the prediction of the mean ionic activity coefficient, density, and vapor pressure of the aqueous solutions over a wide range of temperatures and molalities (298–573 K and 0–8 *m*). We note that, salting out of carbon dioxide and methane in saline water was also accurately predicted.

All of the approaches discussed thus far combine the SAFT framework with the primitive model to describe the ionic species. A more accurate, but more complex, approach is to explicitly include ion-dipole interactions in the model by describing the solvent as a dipolar fluid. In this approach, the solvent dielectric is not required as an input to the calculations as it is calculated from the dipole moment within the theory. In his seminal work, Zhao et al. developed an electrolyte version of the SAFT-VR equation - SAFT-VR+DE - based on the fully non-primitive model of electrolytes. The SAFT-VR+DE approach allows the explicit description of the ion-solvent and solvent-solvent interactions between asymmetric ions and the dipolar solvent. During its development, SAFT-VR+DE was tested against isothermal-isobaric ensemble Monte Carlo simulations and the effect of different ion concentrations and different ratios of the cation, anion, and solvent segment diameters on pressure-volume-temperature (PVT) behavior studied. The simulations highlighted the importance of accounting for the size of the ions and accurate values for the solvent dielectric constant. As such, it was shown that the non-primitive model provides a more accurate prediction of the PVT behavior of model electrolyte solutions compared to the more commonly used DH theory and primitive models. In closely related work, Herzog et al.⁷⁹ later combined the PC-SAFT equation of state with the nonprimitive model of electrolytes, with the ions considered to be a mixture of charged hard spheres of the same diameter (i.e., a semi-restricted non-primitive model [SNPM]). The accuracy of the approach, and specifically the ion-dipole interaction term, was validated by predicting the Gibbs free energy of solvation at infinite dilution. The Pauling crystal diameters were used to determine the ion radii and the ion/water dispersion interaction was calculated using the relationship of Mavroyannis and Stephen;⁷² no ion-ion dispersive interactions and fitted parameters were used. Excellent agreement for the Gibbs free energy of solvation with experimental data was obtained for some (particularly similar anionic and cationic sizes such as KF, RbF, CsCl) alkali halide salt solutions, while pronounced deviations were observed for most of the others. The authors suggested that the use of the SNPM, as opposed to the full non-primitive model could be one reason for the observed deviations from experimental data. To achieve a better representation of the macroscopic thermodynamic properties a salt-specific fitted ion diameter and cation-water interaction was included via a SAFT-association term. The ion diameter and association energy parameters were obtained by fitting to the mean ionic activity coefficient and osmotic coefficient of different aqueous electrolyte solutions; however, one should note, that the fitted radii exhibit a reverse size trend in that, for example, LiCl has a larger radii than CsCl. Systematically increasing deviations in the correlated properties were observed as the size of the ions increased, which may be due to the inappropriate ion sizes. Using this approach, vapor pressure and salt densities were predicted and found to be in good agreement with experimental data.

Irrespective of the adopted molecular model, a common aspect of almost all SAFT-based studies of electrolyte solutions is the use of multiple fitted parameters, which overshadows the predictive ability of the approach. Furthermore, with few exceptions^{60,77} these approaches concentrate on determining the mean ionic activities, osmotic coefficients, and solution densities at room temperature and pressure, with no effort made to cover broader arrays of thermodynamic properties such as solvation and dielectric decay. In an effort to develop a more accurate approach, here the non-primitive model-based SAFT-VR+DE equation of state is used to study 19 different 1:1 electrolyte solutions. Emphasis is placed on developing a predictive equation of state that is capable of capturing a wide range (i.e., mean ionic activity, osmotic coefficient to dielectric decay, solvation) of thermodynamic properties and at temperatures beyond standard conditions. Therefore, the number of fitted parameters is minimized and those parameters that are essential to capture the physical interactions identified.

Molecular Model and Theory

In the SAFT-VR+DE approach used in this work,⁴⁶ the solvent is explicitly taken into account as a dipolar associating fluid. The electrolyte solution is therefore described by a mixture of charged ions of arbitrary sizes and dipolar associating molecules, as shown in Figure 1. We first consider only weak electrolyte systems and so a completely dissociated model for the ions is adopted following the work of Zhao et al.⁴⁶ In this case, the ions are described as a mixture of positively and negatively charged hard spheres that interact via Coulombic attraction and hard-sphere repulsion terms. The water molecules are modeled as dipolar associating hard spheres with an embedded dipole and four association sites to capture the H-bonding nature of the water molecule. In addition to the ion-dipole, dipole-dipole and associative interactions between the solvent molecules, a dispersive interaction representing induced dipolar-charge interactions between the cation and solvent has been considered through a SW potential. The potential model for the interaction of the solvent and ionic species is therefore given by

$$u(r) = u^{SW}(r) + u^{CC}(r) + u^{CD}(r) + u^{DD}(r) \quad (1)$$

where u^{SW} , u^{CC} , u^{CD} and u^{DD} are potential model corresponding to SW, charge-charge, charge-dipole and dipole-dipole interactions respectively and defined as,

$$u_{ij}^{SW}(r) = \begin{cases} +\infty & r < \sigma_{ij} \\ -\epsilon_{ij} & \sigma_{ij} \leq r < \lambda_{ij}\sigma_{ij} \\ 0 & r > \lambda_{ij}\sigma_{ij} \end{cases} \quad (2)$$

$$u_{ij}^{CC}(r) = \begin{cases} +\infty & \text{if } r \leq \sigma_{ij} \\ \frac{z_i z_j e^2}{4\pi\epsilon r} & \text{if } r > \sigma_{ij} \end{cases} \quad (3)$$

$$u_{ij}^{CD}(r) = \begin{cases} +\infty & \text{if } r \leq \sigma_{ij} \\ \frac{z_i e \mu}{4\pi\epsilon r^2} (\hat{r} \cdot \hat{n}) & \text{if } r > \sigma_{ij} \end{cases} \quad (4)$$

and

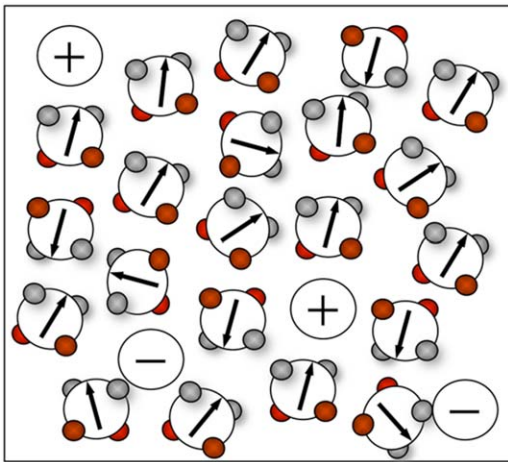


Figure 1. Schematic representation of the molecular model used in the SAFT-VR+DE approach to describe electrolyte solutions.

The model shown considers ions in an associating dipolar solvent with the ionic species completely dissociated. [Color figure can be viewed in the online issue, which is available at wileyonlinelibrary.com.]

$$u_{ij}^{DD}(r) = \begin{cases} +\infty & \text{if } r \leq \sigma_{ij} \\ -\frac{\mu^2}{4\pi\epsilon r^3} D(\mathbf{n}_1 \mathbf{n}_2 \hat{\mathbf{r}}) & \text{if } r > \sigma_{ij} \end{cases} \quad (5)$$

where

$$D(\mathbf{n}_1 \mathbf{n}_2 \hat{\mathbf{r}}) = 3(\mathbf{n}_1 \cdot \hat{\mathbf{r}})(\mathbf{n}_2 \cdot \hat{\mathbf{r}}) - \mathbf{n}_1 \cdot \mathbf{n}_2 \quad (6)$$

Here, ϵ_{ij} and λ_{ij} are the depth and width of the SW dispersive pair potential between molecules i and j and $\sigma_{ij} = (\sigma_i + \sigma_j)/2$ with σ_i and σ_j being the hard core diameter of molecules i and j . In the above expression for the function D , $\hat{\mathbf{r}}$ is the unit vector in the direction of r joining the center of the segments and $\hat{\mathbf{n}}_i$ is a unit vector parallel to the dipole moment of segment i , the index n denotes the dipolar solvent molecule and z_i and μ are the charge of ion i and dipole moment of the solvent molecule, respectively. The model outlined above is used to describe electrolyte solutions at low and moderate salt concentrations (from 0 to 6 mol/L). Of particular interest in our work is the study of mixed solvent electrolytes for which most experimental data lies below the concentrations of 6 m . The model parameters have therefore been developed with the goal of providing a good representation of electrolyte solutions up to concentrations of 6 m . At higher concentrations ($>6 m$), the model parameters have been used to predict the thermodynamic properties, and if needed, ion association is also considered. As the ionic concentration increases, the dielectric of the solvent media decreases, allowing more interaction between ionic species and the formation of ion pairs.^{80–82} Thus including ion association at higher salt concentrations provides a more realistic model of these systems and a better theoretical representation of the experimental results.

In the SAFT-VR+DE theoretical framework, the Helmholtz free energy³⁸ of an electrolyte solution is given by

$$\frac{A}{Nk_bT} = \frac{A^{\text{ideal}}}{Nk_bT} + \frac{A^{\text{mono}}}{Nk_bT} + \frac{A^{\text{assoc}}}{Nk_bT} + \frac{A^{\text{ion-assoc}}}{Nk_bT} \quad (7)$$

where, N is a total number of molecules, k_b is the Boltzmann constant, T is temperature, and A^{ideal} , A^{mono} , and A^{assoc} are the

free energy contributions due to the ideal, monomer, and association interactions, respectively. For concentrated electrolyte solutions, the free energy contribution due to the presence of association between the ions, $A^{\text{ion-assoc}}$, is also included. Since all of the molecules considered in this work are monomeric species, we omit the free energy contribution due to chain formation.

The ideal Helmholtz free energy of a mixture of n components is given by

$$\frac{A^{\text{ideal}}}{Nk_bT} = \sum x_i [\ln(\rho x_i \Lambda_i^3) - 1] \quad (8)$$

where ρ is the molecular number density, x_i is the mole fraction, and Λ the thermal de Broglie wavelength of species i , which incorporates the kinetic (translational, rotational, and vibrational) contributions to the partition function of the molecule.

The contribution to the Helmholtz free energy due to the interactions between monomer segments is given as

$$\frac{A^{\text{mono}}}{Nk_bT} = \frac{A^{\text{sw}}}{Nk_bT} + \frac{A^{\text{el}}}{Nk_bT} \quad (9)$$

where, A^{sw} and A^{el} are the free energy contribution due to the SW dispersion and electrostatic interactions, respectively.

$$\frac{A^{\text{sw}}}{Nk_bT} = \left(\sum x_i m_i \right) \frac{A^{\text{sw}}}{N_s k_b T} = \left(\sum x_i m_i \right) a^{\text{sw}} \quad (10)$$

The monomer free energy per segment of a mixture a^{sw} is obtained as in the original SAFT-VR approach from a second-order high temperature perturbation expansion⁸³

$$a^{\text{sw}} = a^{\text{hs}} + \beta a_1 + \beta^2 a_2 \quad (11)$$

where $\beta = (1/k_bT)$, a^{hs} is the free energy contribution due to the reference hard sphere system and a_1 and a_2 are the first two perturbation terms associated with the attractive energy.

A^{el} is determined using the MSA for mixtures of ions and dipoles developed by Blum and Wei.^{40,84} Within the MSA, the expression for the electrostatic free energy is given by

$$\frac{A^{\text{el}}}{Vk_bT} = \frac{E^{\text{el}}}{Vk_bT} - J - J' \quad (12)$$

where, V is the total volume of the solution, E^{el}/Vk_bT is an internal energy per unit volume and J and J' functionals of the MSA closure condition. Details of these terms can be found in Appendix B.

The contribution to the free energy due to the associative (short-ranged attractive) nature of the molecules is given by⁴⁷

$$\frac{A^{\text{assoc}}}{Nk_bT} = \sum x_i \left[\sum \left(\ln X_{a,i} - \frac{X_{a,i}}{2} \right) + \frac{s_i}{2} \right] \quad (13)$$

where, the first sum is over the number of species present in the system and the second sum is over all sites s_i of type a in a molecule corresponding to species i . $X_{a,i}$ represents the fraction of molecules of species i that are not bonded at site a and satisfies the mass action law,

$$X_{a,i} = \frac{1}{1 + \sum \sum \rho x_j X_{b,j} \Delta_{a,b,i,j}} \quad (14)$$

where

$$\Delta_{a,b,i,j} = K_{a,b,i,j} f_{a,b,i,j} g_{ij}^M(\sigma_{ij}) \quad (15)$$

$$f_{a,b,i,j} = \exp(-\varepsilon_{a,b,i,j}/kT) - 1 \quad (16)$$

The function $\Delta_{a,b,i,j}$ characterizes the association between site a on molecule i and site b molecule j ; $f_{a,b,i,j}$ is the Mayer f function for the a - b site-site interaction with bonding energy $\varepsilon_{a,b,i,j}$ and volume $K_{a,b,i,j}$ available for bonding. g^M is the monomer-monomer radial distribution, which for water association is mediated by four dispersive SW association sites and is given by

$$g^M = g_{ij}^{SW} = g^{hs}(\sigma_{ij}) + \beta \varepsilon_{ij} g_1(\sigma_{ij}) \quad (17)$$

as in the original SAFT-VR approach.⁸³ Here, g^{sw} and g^{hs} are the contact values of the radial distribution function (RDF) for square-well and hard sphere interactions respectively and g_1 the first order perturbation term. Ions are regarded as having one association (charged SW dispersive) site and so the monomer-monomer radial distribution becomes

$$g^M = g_{ij}^{CSW} = g^{SW}(\sigma_{ij}) \left(1 + g_{ij}^{el}(\sigma_{ij}) \right) \quad (18)$$

where, the contact value RDF for Coulombic charged interactions, g_{ij}^{el} , is obtained from the MSA as⁸⁴

$$g_{ij}^{el}(\sigma_{ij}) = \frac{-D_i^F D_j^F}{4\pi\sigma_{ij}} \left\{ \frac{\rho_n \sigma_n^2 V_\eta^2}{D\beta_6^2(\sigma_n + \lambda\sigma_i)(\sigma_n + \lambda\sigma_j)} + \frac{4\Gamma_i^s \Gamma_j^s}{DD_{ac}} \right\} \quad (19)$$

where ρ_n is a density of dipolar solvent particles and the expressions for the screening parameter Γ^s and the remaining terms in equation 19 are given in appendix B.

Results and Discussion

Water

Water molecules are modeled as SW dispersive hard spheres with a dipole moment embedded in the center of the sphere and four short-range attractive SW sites to describe association interactions that mimic hydrogen bonding, as in earlier work.⁸⁵ Although it is well known that the value of the water dipole moment varies significantly from the gas to the liquid phase and the gas-phase dipole moment for water⁸⁶ is well characterized, the liquid phase moment is not as well defined. A wide range of values have been reported in the literature from both experimental and theoretical studies, with the most commonly accepted value being 2.6 D due to Coulson and Eisenberg.⁸⁷ However, far-IR vibration-rotation-tunneling spectroscopy along with accurate *ab initio* calculations have shown that the liquid phase dipole moment depends upon the cluster size and can have a value as high as 2.7 D.⁸⁸ Since a variable dipole moment cannot be used in the theory, and in the study of electrolyte solutions we are primarily concerned with liquid water, we have reparameterized the original SAFT-VR+D water model that was fitted with a dipole moment of 1.8 D. As can be seen from Figure 2, when a dipole moment of 2.18 D is used the theory provides a good representation of the liquid water phase dielectric at room temperature and pressure. Hence an effective dipole moment of 2.18 D that takes into account the actual dipole moment of an isolated water molecule (1.80 D) and the effect of polarizability induced by neighboring water molecules was chosen. We note that the dipole moment used is lower than the typically reported values for the liquid phase due to the fact that dispersion energy parameters also partially take into account induced polarizability effects. The remaining model parameters [i.e., the hard-core diameter (σ), SW potential depth (ε) and

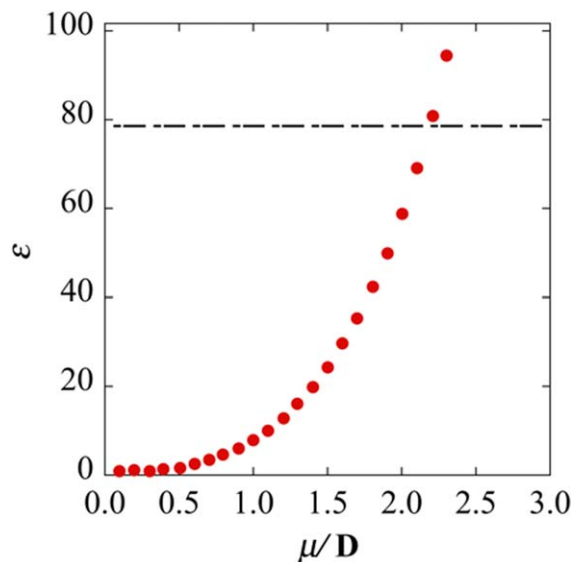


Figure 2. Change in the dielectric constant ε as a function of dipole moment μ for water as predicted by the SAFT-VR+D equation of state at room temperature (298.15 K) and pressure (0.101325 MPa).

Dashed line represents the dielectric constant for water as reported in experimental studies,⁶¹ [Color figure can be viewed in the online issue, which is available at [wileyonlinelibrary.com](http://www.wileyonlinelibrary.com).]

range (λ), association energy (ε^{HB}) and bonding volume (κ^{HB})] were obtained by fitting to experimental vapor pressure and saturated liquid density data between 290 and 595 K.⁸⁹ Experimental data close to the critical region (around 10%) have been excluded from the fitting procedure, as SAFT-VR+D like other analytical equation of state exhibits classical behavior in the critical region and so over predicts the critical point.⁹⁰ Additionally, data points near the triple point have also been excluded since it has been shown that inclusion of such data can distort the results.⁹¹ Simulated annealing^{92,93} is used to fit the model parameters with an objective function defined as a function of vapor pressure and saturated liquid density as given in Appendix A. The resulting parameters are presented in Table 1, and as can be seen from Figure 2, the theory provides a good representation of the dielectric constant of water at room temperature and pressure while also capturing the phase behavior (Figure 3). The AAD over the whole phase diagram is 1.49% for the vapor pressures and 2.43% for the saturated liquid densities using the SAFT-VR+D equation of state. We note that the %AADs are comparable to those obtained in our previous work (%AADP 0.92 and %AAD ρ 2.87),⁸⁵ in which a dipole moment of 1.8 D was used, while giving us a more accurate description of the saturated liquid densities that are essential for liquid phase characterization. As expected, and can be seen from Figure 3, SAFT-VR+D overpredicts the critical region of the phase diagram^{94,95} and does not capture the experimentally observed density maximum of water at lower temperature as a temperature-dependent segment diameter is not used.⁹⁶

Electrolytes

In this work, several 1:1 alkali halide salts have been studied. The salts are modeled as charged hard spheres of asymmetric size. In any study of electrolytes, the concept of “ionic radius,” which depends upon the valence, electronic spin state,

Table 1. SAFT-VR+DE Parameters for Water and the % AAD in Vapor Pressure and Saturated Liquid Density as Compared to Experiment⁸⁹

	μ (D)	σ (nm)	ϵ/k_b (K)	λ	m	ϵ^{HB}/k_b (K)	K^{HB} (nm ³)	%AAD p	%AAD ρ_{liq}
H ₂ O	2.179	0.3002879	312.3598	1.529558	1	758.5521		1.49	2.43

and coordination number of the ions, is a central one.⁹⁷ Goldschmidt⁹⁸ was the first to propose a limited set of crystal ionic radii on the basis of interatomic distances. Subsequently, Pauling⁹⁹ recommended sets of radii for monoatomic ions, measured from the spatial proportion occupied by the ions within the salt crystal based on assuming a coordination number of six. Later, Shannon^{97,100} proposed a list of revised effective ionic radii and crystal ionic radii to include more unusual oxidation states and coordinations using a more extensive set of experimental data on intermolecular distances, empirical bond length-bond strength relations, etc. These Pauling-type ionic radii, although common and widely used, are not the only ones that have been proposed. For example, Gourary and Adrian¹⁰¹ and Levy and Danford¹⁰² recommended new sets of ionic radii by redefining the cation-anion distances. More recently, Mähler and Persson¹⁰³ studied the hydrated structures of several different alkali metals using large angle x-ray scattering (LAXS) and double difference infrared spectroscopy and proposed a set of ionic radii for Li, Na, K, Rb, and Cs ions in aqueous solution that corresponded to newly determined coordination numbers. The RDFs obtained from the LAXS experiments indicated coordination numbers of 6, 7, and 8 for Na, K, and Cs ions, respectively. A coordination number of 8 was suggested for Rb and 4 for lithium. In this study, the cationic radii have been taken from the work of Mähler and Persson¹⁰³ and for anions, the effective ionic radii proposed by Shannon,^{97,100} which correspond to a coordination number of six,¹⁰⁴ have been used.

Ionic species in the electrolyte solution interact via charge-charge and charge-dipole interactions. Additionally, a salt-specific dispersion interaction between the cation and the solvent was considered to capture the nonelectrostatic-induced dispersive effect. Initially, no dispersion interaction between the anion and solvent was included in the model. The unlike cross dispersion interaction energy ($\epsilon_{\text{cation-H}_2\text{O}}$) between the cation and solvent is obtained by fitting to the mean ionic activity coefficient data at 298.15 K and 0.101325 MPa using the Levenberg–Marquardt¹⁰⁵ algorithm. The dispersive SW interaction range (λ) for the cations was fixed at 1.2.^{60,106} The Lorentz–Bethelot combining rule has been used to determine the cross-interaction range parameters between the cations and solvent molecules

$$\lambda_{\text{H}_2\text{O-cation}} = \frac{\sigma_{\text{H}_2\text{O}}\lambda_{\text{H}_2\text{O}} + s_{\text{cation}}\lambda_{\text{cation}}}{\sigma_{\text{H}_2\text{O}} + \sigma_{\text{cation}}} \quad (20)$$

It was observed during the fitting process that a reasonable theoretical representation of the experimental mean ionic activity coefficient data could not be obtained for several salts containing Li⁺, Na⁺, and F⁻ ions using the ionic radii proposed by Mähler et al. (the % AAD obtained is reported in Table A1 of the appendix material). These small ions are considered to be net structure makers, which implies that they distort the water structure around them over multiple water shells.^{107,108} As a result, the use of a larger diameter for Li⁺, Na⁺, and F⁻ ions, better captures the induced effect on the surrounding water molecules. The diameters for these

ions were therefore obtained from the fitting process alongside the dispersion energy between the cations-water. The approach therefore requires two fitted parameters for ten of the aqueous salt solutions studied and only one for the remaining nine. We note, that although the radii of some of the ions is now fitted, this does not disrupt the trend in the values for the ionic radii, that is, Li < Na and F < other anions. The final values of the ionic radii used in this study are reported in Table 2. We also note that the proposed radii for Li and Na fall between the ionic radii proposed by Mähler et al. and the van-der-Waals radii, which corresponds to the

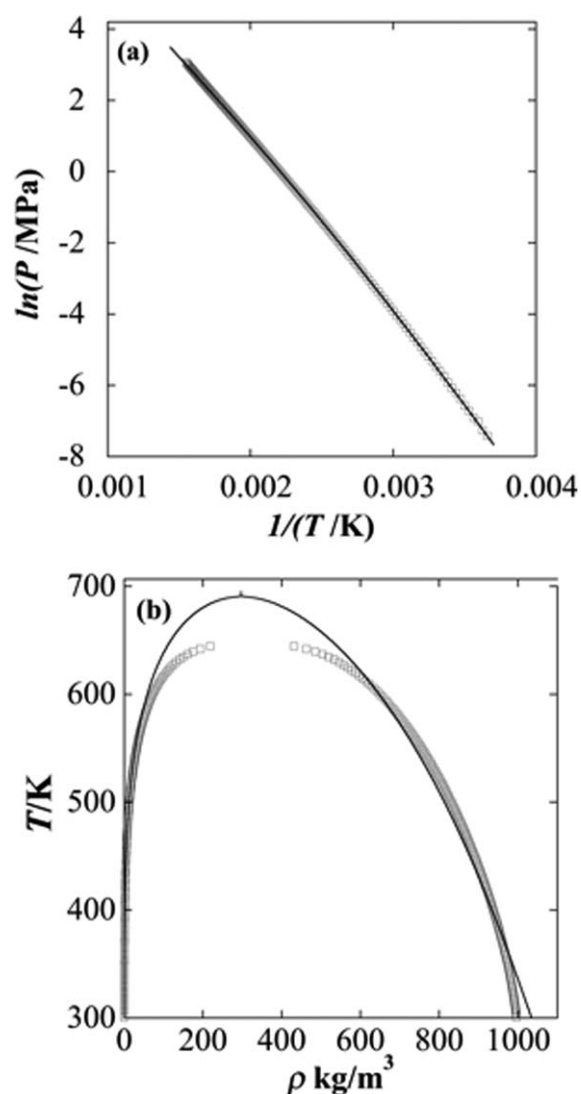


Figure 3. Comparison of (a) vapor pressure and (b) vapor-liquid coexisting densities for water from the SAFT-VR+D equation of state and experiment.

Symbols represent the experimental data and the theory is represented by the solid line.⁸⁹

Table 2. Ion-Specific SAFT-VR+DE Diameter (σ_{ion}) and SW Dispersion Range (λ_{ion}) Parameters for the Alkali and Halide Ions Studied

	Li	Na	K	Rb	Cs	F	Cl	Br	I
σ_{ion} (nm)	0.265	0.28	0.292	0.328	0.346	0.332	0.362	0.392	0.44
λ_{ion}	1.2	1.2	1.2	1.2	1.2	–	–	–	–

dispersive interactions. In Table 3, we report the binary salt-specific cation-H₂O dispersion interaction parameters obtained from fitting to experimental mean ionic activity coefficient data at 298.15 K and 0.101325 MPa and the corresponding AADs from the experimental data over the specified molality range.

In Figure 4, selected results for the mean ionic activity coefficient of different salts are presented. As can be seen from the figure, we have been able to obtain a good representation of the experimental data up to 6 *m* salt concentration. It can be noted that as the anion size increases for a specific alkali cation, larger deviations are seen compared to the smaller anions studied, particularly at higher salt concentrations. This may be due to the exclusion of dispersion interactions between the anions and water molecules, which plays a greater role with increasing ion concentration and will be further discussed later.

Using the parameters determined, other thermodynamic properties of the aqueous electrolyte solutions studied, such as osmotic coefficient, water activity coefficient, and density, were then predicted at 298.15 K. The predicted osmotic coefficients for the 19 different salts studied were found to be in good agreement with the experimental data (%AADs are reported in the Table A2 of the Appendix), especially considering the approach uses only a single fitted salt-specific parameter. We also note that the predicted results for the osmotic coefficients are well within the range of %AAD reported by Herzog et al.,⁷⁹ who correlated the osmotic coefficient, although in our case a smaller molality range has been studied.

Table 3. Salt-Specific Dispersion Energy Parameters for the Cation-Solvent ($\epsilon_{\text{cation-H}_2\text{O}}$) Interaction for the Different Electrolytes Studied and the %AAD for the SAFT-VR+DE Equation of State for γ_{\pm} as Compared to Experimental Data¹⁰⁹ at 298.15 K and 0.101325 MPa Over the Molality Range Specified

Salts	$\epsilon_{\text{cation-H}_2\text{O}}$	% AAD γ_{\pm}	Molality (mol/kg)
LiCl	1770.968	8.51	0.1–6.0
LiBr	1606.255	5.86	0.1–6.0
LiI	1444.732	9.18	0.1–3.0
NaF	1732.250	0.93	0.1–1.0
NaCl	1382.396	8.03	0.1–6.0
NaBr	1274.406	3.53	0.1–4.0
NaI	1209.249	9.78	0.1–3.5
KF	1478.095	8.64	0.1–4.0
KCl	1189.358	4.60	0.1–4.5
KBr	1087.631	3.10	0.1–5.5
KI	1067.243	9.09	0.1–4.5
RbF	1043.135	4.95	0.1–3.5
RbCl	863.759	2.42	0.1–5.0
RbBr	826.077	5.66	0.1–5.0
RbI	858.326	12.1	0.1–5.0
CsF	919.569	1.69	0.1–3.5
CsCl	749.444	5.70	0.1–6.0
CsBr	734.455	9.11	0.1–5.0
CsI	760.645	8.55	0.1–3.0

In Figure 5, the predicted osmotic coefficient (Φ) for different salts from 0 to 6 *m* are presented. Good agreement for different Li salts in comparison with experimental data is found as shown in Figure 5a. As can be seen from Figure 5b, for some of the salts studied, such as NaCl, the theory overpredicts the osmotic coefficient at high salt concentrations. We believe this is due to the presence of ion association¹¹¹ and an effort has been made to incorporate this behavior into the theory through the inclusion of an association term, as discussed further below.

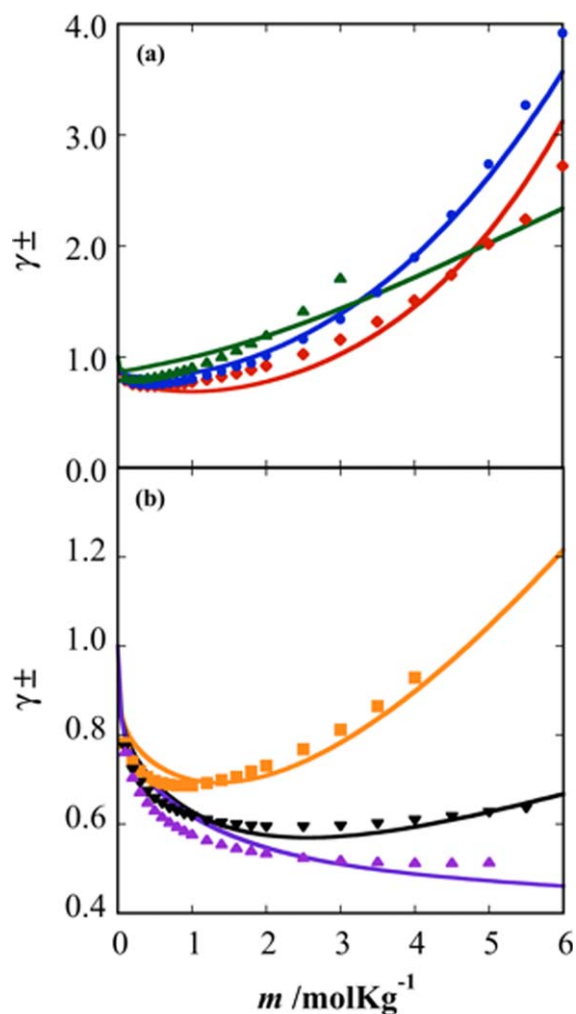


Figure 4. Mean ionic activity co-efficient of (a) LiCl (red \diamond), LiBr (blue \bullet), LiI (green \blacktriangle) and (b) NaBr (orange \blacksquare), KBr (black \blacktriangledown), RbBr (purple \blacktriangle) at 298.15 K and 0.101325 MPa.

Symbols represent the experimental data¹⁰⁹ and solid lines the theoretical correlations from the SAFT-VR+DE equation of state. [Color figure can be viewed in the online issue, which is available at wileyonlinelibrary.com.]

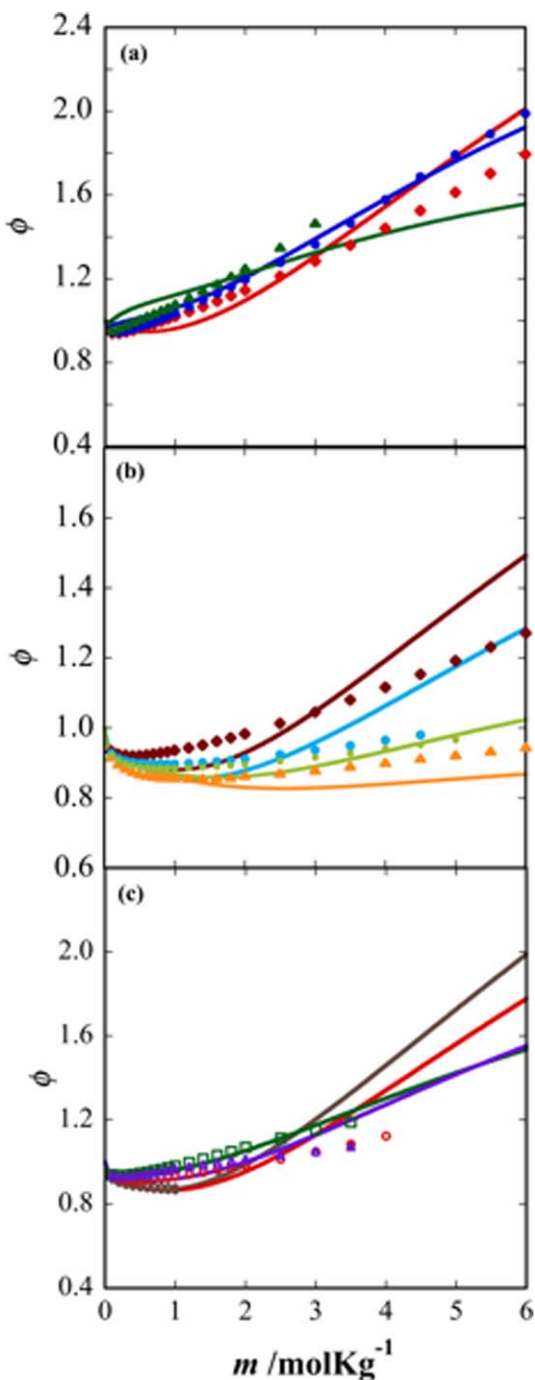


Figure 5. Aqueous osmotic coefficient of (a) LiCl (red \blacklozenge), LiBr (blue \bullet), LiI (green \blacktriangle) and (b) NaCl (brown \blacklozenge), KCl (blue \blacktriangledown), RbCl (green \bullet), CsCl (orange \blacktriangle), (c) NaF (brown \blacklozenge), KF (red \circ), RbF (purple \blacktriangle), CsF (green \square) at 298.15 K and 0.101325 MPa.

Symbols represent the experimental data¹⁰⁹ and solid lines predictions from the SAFT-VR+DE equation of state. [Color figure can be viewed in the online issue, which is available at wileyonlinelibrary.com.]

Gibbs free energy of solvation

Upon dissolving a salt in water, the ions are surrounded by the water and form a hydrogen-bonded network with neighboring water molecules; the energy released during this process is termed the free energy of solvation. As one might expect, an implicit treatment of the solvent at the primitive model level

fails to capture this phenomena. For example, using the salt parameters proposed in the SAFT-VRE approach,⁵⁷ the predicted Gibbs free energy of hydration (ΔG^{hyd}) shows large deviations from experimental data as presented in Table A3. We note that while the recently modified SAFT-VRE by Schreckenberget al.⁶⁰ improves the trend in the free energy of solvation, significant deviations from the experimental values are still observed. With the solvent treated as a dielectric continuum, it is difficult to obtain even qualitative agreement with experimental results. In the non-primitive model, as used in this study, the solvent molecules are explicitly included and so the ion-solvent interactions are described by an explicit ion-solvent term. This provides a theoretical advantage in terms of capturing the solvation behavior compared to the implicit solvent models frequently adopted in SAFT-based equations of state for electrolyte solutions. In Table 4, ΔG^{hyd} as calculated from the SAFT-VR+DE equation of state for individual ions (cations and anions) and salts are presented and compared with experimental data.¹⁰⁹ Note that ΔG^{hyd} for the cations varies with the salts due to the use of salt-specific water-cation dispersion energy parameters. From the table it can be seen that, while the theory provides a very good representation of the hydration energy for cations, deviations are seen in the predictions for the anions. This can be explained by the fact that at infinite dilution ionic concentrations the number of water molecules surrounding the anions increases considerably compared to moderate or high concentration. In this scenario, the anions will experience dispersion interactions with solvent, the neglect of which could be one reason behind the observed deviations.

As discussed previously, Herzog et al. investigated the Gibbs free energy of hydration using the SNPM model.⁷⁹ Along with the dipolar and ionic interactions, dispersive interactions between both the cation and anion and water were considered. Although, higher deviations were observed from the experimental results for some of the cations, most of the anions were in good agreement. They also commented that the use of a fully non-primitive model, which captures the individual sizes of the cations and anions, might bring improvement to the predictions. Here, we report that significant improvements are achieved for cations Na, K, Rb, and Cs in terms of the Gibbs free energy of hydration but some deviations have been observed for the anions, which again we believe is due to not considering the anion-solvent dispersive interactions. Irrespective of the deviations observed, we can however conclude, that the results predicted using the non-primitive or SNPM models are still more accurate than any result obtained using a primitive model approach (as demonstrated in Table A3 in the Appendix).⁴⁵

Effect of ions on the dielectric properties of water

The interactions between charged ions and dipolar solvent molecules play an important role in determining the thermophysical properties of electrolyte solutions. Over the years, although many SAFT-based equation of state based on the primitive model^{57,59,66,67} for electrolyte solutions have been proposed and found to be able to capture the essential thermodynamic properties of these systems, such as the mean ionic activity coefficient, osmotic coefficient, and density, they are unable to capture the variation of the dielectric constant of the solvent with salt concentration. Generally, in primitive models the dielectric constant is fixed over the whole salt concentration range studied, whereas the dielectric constant of the solvent is experimentally a function of the salt concentration (i.e., the dielectric properties are reduced as the salt concentration

Table 4. Comparison Between Experiment¹⁰⁹ and the SAFT-VR+DE Equation of State Predictions for the Gibbs Free Energy of Hydration for Different Electrolyte Solutions

Salt	ΔG^{hyd} Cation (KJ/mol)	ΔG^{hyd} Cation Expt. (KJ/mol)	ΔG^{hyd} Anion (KJ/mol)	ΔG^{hyd} Anion Expt. (KJ/mol)	ΔG^{hyd} Salt (KJ/mol)	ΔG^{hyd} Salt Expt. (KJ/mol)	%AAD ΔG^{hyd} Salt
LiCl	-464.72	-529.4	-228.35	-304	-693.08	-833.4	16.7
LiBr	-451.43	-529.4	-200.78	-277.7	-652.21	-807.1	19.1
LiI	-438.51	-529.4	-157.66	-242.6	-596.17	-772	22.9
NaF	-455.83	-423.7	-256.97	-429.1	-712.79	-852.8	16.4
NaCl	-425.42	-423.7	-228.35	-304	-653.77	-727.7	10.2
NaBr	-416.14	-423.7	-200.78	-277.7	-616.92	-701.4	12.1
NaI	-410.58	-423.7	-157.66	-242.6	-568.23	-666.3	15.0
KF	-428.63	-351.9	-256.97	-429.1	-685.59	-781	12.6
KCl	-402.20	-351.9	-228.35	-304	-630.55	-655.9	4.5
KBr	-392.99	-351.9	-200.78	-277.7	-593.77	-629.6	6.4
KI	-391.15	-351.9	-157.66	-242.6	-548.81	-594.5	8.7
RbF	-370.34	-329.3	-256.97	-429.1	-627.31	-758.4	17.4
RbCl	-343.03	-329.3	-228.35	-304	-579.39	-633.3	8.8
RbBr	-339.00	-329.3	-200.78	-277.7	-547.79	-607	10.1
RbI	-342.44	-329.3	-157.66	-242.6	-508.11	-571.9	11.7
CsF	-348.36	-306.1	-256.97	-429.1	-605.33	-735.2	17.2
CsCl	-328.52	-306.1	-228.35	-304	-556.87	-610.1	8.3
CsBr	-326.78	-306.1	-200.78	-277.7	-527.55	-583.8	9.2
CsI	-329.82	-306.1	-157.66	-242.6	-487.47	-548.7	11.0

increases, due to ionic polarizability, and the water structure modified due to the formation of hydration shells that restrict the rotation of free water molecules).^{24,113,114} Implementation of a more advanced level of theory, such as a non-primitive model that can capture the underlying physics of these complex phenomena, should provide an approach that is better equipped to describe this dielectric decay phenomena. We note that although Herzog et al.⁷⁹ applied the SNPM in their study they do not examine the ability of the theory to capture the correct dielectric behavior. In this study, we report for the first time the decay of the dielectric constant in the presence of ions using a SAFT-based equation of state.

The dielectric constant of the solution has been obtained following the work of Wei et al.⁸⁴ as

$$\epsilon_A = 1 + \frac{\rho_n \alpha_2^2 \beta_6^2 (1 + \lambda)^4}{16} \quad (21)$$

where $\alpha_2^2 = 4\pi\beta\mu^2/3$, $\lambda = \beta_3/\beta_6, \beta_3 = 1 + b_2/3$, and $\beta_6 = 1 - b_2/6$ and α_2^2 and b_2 are the dipole-dipole strength parameters obtained when solving the MSA equations (see Appendix B). In Figure 6, we compare the experimental and predicted dielectric constant for different electrolyte solutions. From Figure 6a, which reports the dielectric constant for five salts with different cations (Li, Na, K, Rb, and Cs) and the same chloride anion, we find that both the theory and experimental values do not show any dependence on the size of the cation and that a decreasing asymptotic trend in the dielectric permittivity is observed that is well captured by the theory. This is consistent with other work indicating dielectric decay is more dependent on cationic charge than size.¹¹⁷ In Figure 6b, a comparison between the theoretical predictions and experimental dielectric constant for KF and NaI is presented. As the size asymmetry between the anion and cation increases with larger anion size, the dielectric depression increases, with the trend in the experimental data again well captured by the theory. In both cases, the theory is only in qualitative agreement with experiment, in that it captures the correct trends, but deviates from the experimental values. Some inaccuracy in the theoretical predictions could be due to the approximations adopted when the expressions for the pair correlation functions and thermodynamics were developed by Wei and Blum.⁸⁴ Specifically, the proposed

solution of the MSA is stated to be only valid for ions of similar size and at low ionic concentration ($<3 m$), with several of the expressions, including pair correlation functions, only tested at low ionic concentrations (i.e., 0.1 and 1 m). Deviations are, therefore, perhaps to be expected when dealing with ions of asymmetric sizes and at the higher ionic concentrations considered in this work. A further issue is the orientation of the water molecules in the hydration shell and the presence of ion-pairs. For salts such as NaCl and CsCl, experiments and simulations confirm the existence of both contact and solvent separated ion pairs.^{81,82} The existence of solvent separated ion pairs at low ion concentrations effectively reduces the number of ions in the solution, which in turn behave more like dipolar molecules and hence increase the dielectric constant of the solvent. This effect is not well captured by the theory as a fully dissociated model is being used and inclusion of the ion-association term discussed below would not improve the situation as the dielectric is calculated from the ion-dipole and dipole-dipole free energy contribution expressions, which are not affected by ion association. We also note however, that the experimentally measured static permittivity of polar conducting fluids such as aqueous electrolytes is known to contain systematic errors due to dielectric saturation and kinetic depolarization and can result in a 25–75% decrease in the measured static permittivity.¹¹⁸ Such a decrease in the experimental static permittivity would increase the accuracy of the theoretical predictions considerably.

Temperature effect on thermodynamic properties of electrolytes

In this section, the effect of temperature on the thermodynamic properties of the electrolyte solutions studied is considered. In Figure 7, the predicted solution densities for KBr and KCl are presented over a wide range of temperatures. From the figure, we can see that the theory accurately captures the behavior of the solution density as a function of temperature. In Figure 7b, we observe a slight (less than 5%) deviation of the theoretical predictions from the experimental data for KCl. We note that the density is a predicted property and that similar deviations in density are commonly seen with SAFT-based equation of states for electrolytes, even though in most cases

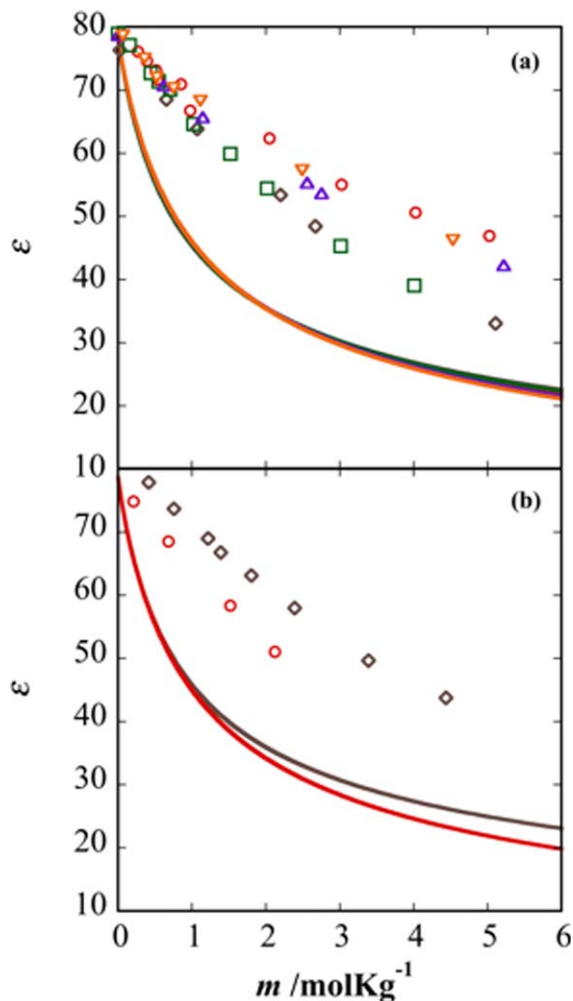


Figure 6. Water dielectric constant for different salt solutions (a) LiCl (gray \diamond), KCl (red \circ), NaCl (green \square), RbCl (purple \triangle), CsCl (orange ∇) and (b) KF (gray \diamond), NaI (red \circ) at 298.15 K temperature and 0.101325 MPa pressure.

Symbols represent the experimental data^{115,116} and solid lines the theoretical predictions. [Color figure can be viewed in the online issue, which is available at wileyonlinelibrary.com.]

the density was included in the fitting process. At low temperatures in the pure limit, the observed deviations from experimental results (apparent from Figure 7b), are due to the over prediction of the saturated liquid density of pure water. Overall, we can conclude that the SAFT-VR+DE approach with a single fitted parameter at 298.15 K and 1 bar for KCl and KBr salts, describes the solution densities well over a range of temperatures (293.15–423.15 K).

We now consider the temperature and pressure dependence of the mean ionic activity coefficient and osmotic coefficient, which are more temperature sensitive properties. In Figures 8 and 9, respectively, the predicted mean ionic activity coefficient and osmotic coefficient for NaCl and NaBr over a temperature range from 298.15 to 573.15 K at saturation pressures are presented. As can be seen from the figures, while the SAFT-VR+DE equation of state is able to capture the correct trend in the mean ionic activity coefficient and osmotic coefficient a function of temperature, the predictions are not in quantitative agreement. As previously discussed, the dipole

moment for water used in the calculations is one that accurately captures the dielectric constant of water at room temperature and pressure. If we consider the behavior of the pure solvent dielectric as a function of dipole moment, as shown in Table 5, it can be observed that although a dipole of 2.18 D works well at room temperature, it underpredicts the dielectric constant at higher temperatures and pressures. In this scenario, if we use a higher dipole moment in the theoretical calculations, without altering/refitting the SAFT-VR+D water parameters, the theory more accurately captures the dielectric of water at higher temperatures and pressures. In the subsequent rows of the table, the value of the dipole moment that predicts a dielectric constant that most closely matches the experimental dielectric data is reported. We note that the dipole moment increases with temperature and pressure due to the fact that the theory underpredicts the dielectric and so a larger effective dipole moment is needed to compensate.

To determine the effect of capturing the correct solvent dielectric on the prediction of the thermodynamic properties, the appropriate values of the dipole moment from Table 5 has

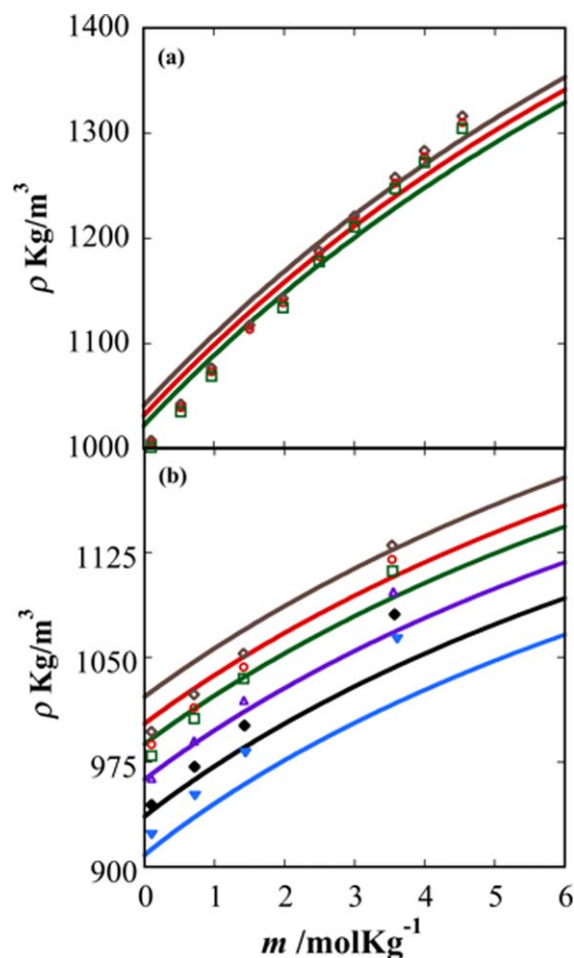


Figure 7. Densities of aqueous solution of (a) KBr at 293.15 K (gray \diamond), 303.15 K (red \circ), 313.15 K (green \square) and (b) KCl at 313.15 K (gray \diamond), 333.15 K (red \circ), 348.15 K (green \square), 373.15 K (purple \triangle), 398.15 K (black \blacklozenge), 423.15 K (blue \blacktriangledown).

Symbols represent the experimental data and solid lines predictions from the SAFT-VR+DE equation of state. [Color figure can be viewed in the online issue, which is available at wileyonlinelibrary.com.]

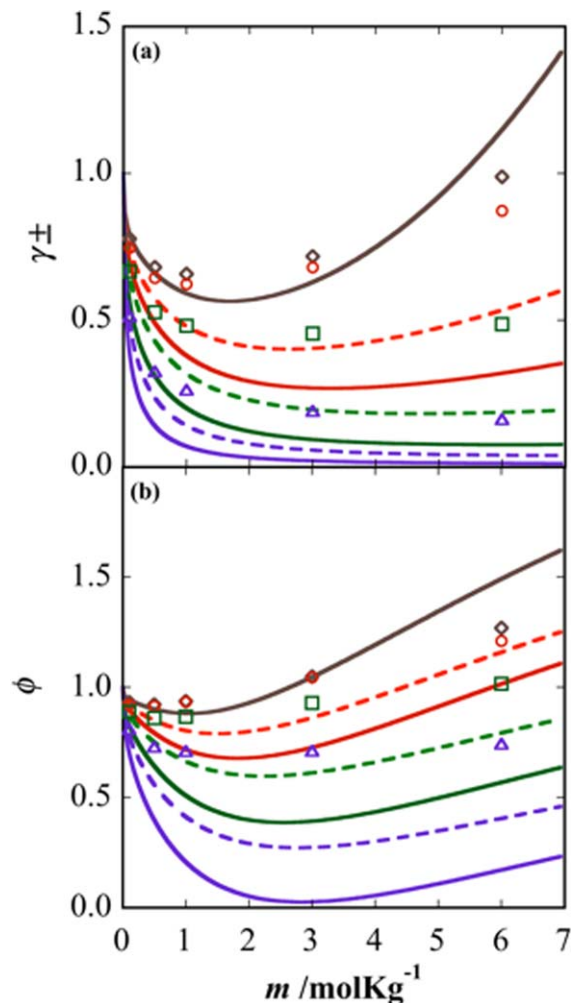


Figure 8. Comparison of the predicted and experimental (a) mean ionic activity and (b) osmotic coefficient for NaCl at 298.15 K/0.1 MPa (gray \diamond), 373.15 K/0.1 MPa (red \circ), 473.15 K/1.55 MPa (green \square), 573.15 K/8.6 MPa (purple \triangle).

The theoretical predictions from the SAFT-VR+DE equation of state with a water dipole moment of 2.18 D are represented by solid lines, while the dashed lines correspond to the theoretical results using the modified dipole moments of 2.25 D (373.15 K) and 2.30 D (473.15/573.15 K). The symbols represent the experimental data.¹¹⁹ [Color figure can be viewed in the online issue, which is available at wileyonlinelibrary.com.]

also been used in the calculations. As can be seen in Figures 8 and 9, the use of the higher temperature and pressure dipole moments has a significant effect on the thermodynamic properties and the accuracy of the theoretical predictions. While deviations between the theoretical predictions and experimental data are still observed, we note that the improvement is achieved simply by changing the dipole moment and without refitting other model parameters. We also note that further deviations are likely due to the fact that the theory underpredicts the solvent dielectric at high salt concentrations, as previously discussed.

Mean ionic activity coefficient at high salt concentrations and ion-association

As the molality in a salt solution increases, the solution dielectric constant decreases considerably due to ion pairing.

While ion pairing is not significant in aqueous solutions of strong electrolytes at ambient temperatures and low salt molality, as the high dielectric constant of water very effectively screens the charge-charge Coulombic interactions, when the salt molality increases charge-charge interactions between the ions become more significant. The average distance between the ions decreases and the ions can form clusters of contact or solvent separated ion pairs in solution.^{80–82,120,121}

For seven of the nineteen salts studied herein, namely NaBr, RbCl, CsCl, KF, LiBr, LiCl, NaI, mean ionic activity coefficient data are available at concentrations higher than 6 m . If the previously determined parameters are used to predict the mean ionic activity coefficient at these higher concentrations, as can be seen in Figure 10, accurate results are obtained for NaBr, RbCl, and CsCl. The dissociated model can therefore be considered to describe the thermodynamic properties of

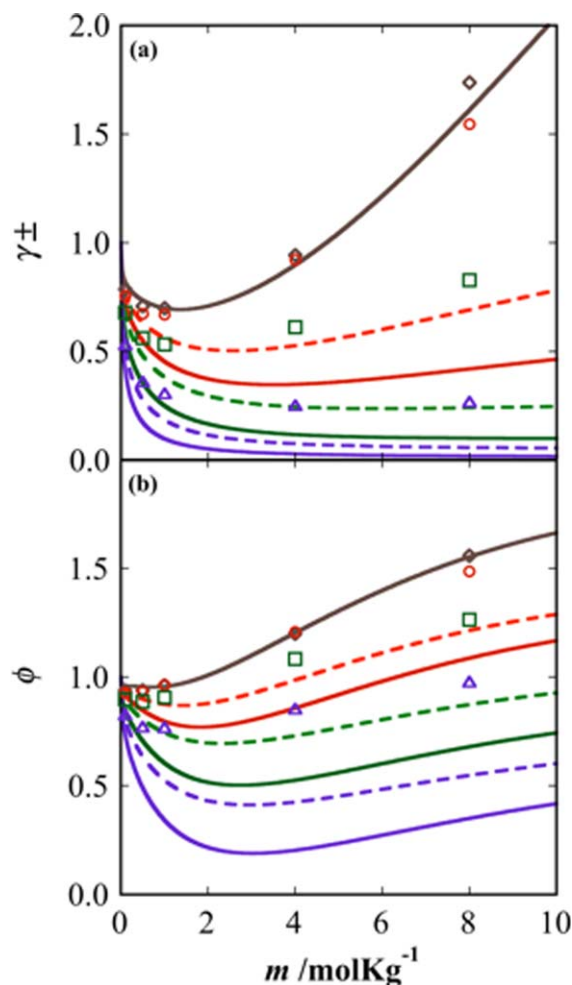


Figure 9. Comparison of the predicted and experimental (a) mean ionic activity and (b) osmotic coefficient for NaBr at 298.15 K/0.1 MPa (gray \diamond), 373.15 K/0.1 MPa (red \circ), 473.15 K/1.55 MPa (green \square), 573.15 K/8.6 MPa (purple \triangle).

The theoretical predictions from the SAFT-VR+DE equation of state with a water dipole moment of 2.18 D are represented by solid lines, while the dashed lines correspond to the theoretical results using the modified dipole moments of 2.25 D (373.15 K) and 2.30 D (473.15/573.15 K). The symbols represent the experimental data.¹¹⁹ [Color figure can be viewed in the online issue, which is available at wileyonlinelibrary.com.]

Table 5. Experimental vs. Theoretically Obtained Dielectric Constant for Different Dipole Moments Calculated Across a Range of Temperature and Pressure

μ (D)	T (K), p (MPa)			
	298.15, 0.1	373.15, 0.1	473.15, 1.55	573.15, 8.6
Expt.	78.58	55.56	34.82	20.10
2.179	78.58	49.93	28.99	16.59
2.250	87.15	55.41	32.28	18.66
2.300	93.57	59.52	34.75	20.23

these four salt solutions well. This is consistent with the molecular simulation study of Fennell et al.,⁸¹ which showed that size symmetric ions compared to size asymmetric ions more readily associate and form contact ion pairs. NaBr, RbCl, and CsCl being asymmetric in size are less prone to ion-pair formation. This is also supported by the conductometric study of Fuoss¹²² who provides further evidence that Rb halide salts are less associative.

If we consider LiCl, LiBr, KF, and NaI, significant deviations from the experimental data are seen in Figure 10 at higher concentrations ($>6 m$). This can be attributed due to other factors such as ion-association or increased ion-solvent interactions, including anion-solvent dispersive interactions, which so far have not been considered in the model but are discussed further below. To better capture the molecular level interactions at higher salt concentrations, ion pairing has been included in the model through the addition of an ion-association term. Although several SAFT-based equation of state^{73,112} have been proposed that consider ion association, they fail to obtain (correlate⁷³ or predict¹¹²) the correct trends with increasing ionic concentrations for properties such as the mean ionic activity coefficient and solution vapor pressure when compared to experimental data. We note, however, that the more recent work of Rozmus et al.⁷⁷ included ion-

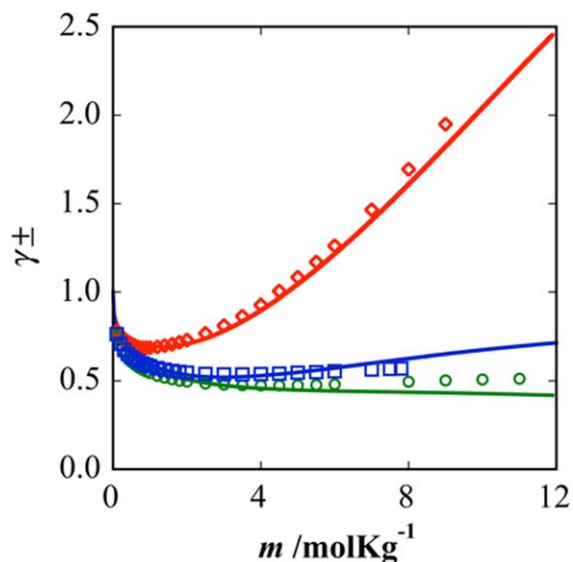


Figure 10. Mean ionic activity coefficient of CsCl (green \circ), RbCl (blue \square), and NaBr (red \diamond) as predicted by the SAFT-VR+DE equation of state (solid lines) compared to experimental data.¹¹⁰

[Color figure can be viewed in the online issue, which is available at wileyonlinelibrary.com.]

association within the molecular model, with the association energy parameter obtained by fitting to experimental mean ionic activity coefficient data at 298.15 K and 1 bar for salt concentrations up to 6 m . Although the theory was able to provide a good correlation of the mean ionic activity coefficient at 298.15 K, an over prediction was observed at higher temperatures. In this study, we investigate whether the inclusion of ion-association in the model improves the theoretical correlations or predictions of the thermodynamic properties at higher salt concentrations.

As discussed above, ion association has been included in the model through a sticky site placed on the charged spherical ions that interact via charged and associative dispersive interactions. To capture the increase in ion interaction and ion-association with the decrease in the dielectric of the medium, the association energy $\epsilon^{\text{ion-assoc}}$ for ions is made dependent upon the solution dielectric constant using the following relation

$$\epsilon^{\text{ion-assoc}} = a - b\epsilon_w^2 \quad (22)$$

where a is obtained by fitting to the experimental mean ionic activity coefficient data at higher concentration ($> 6 m$) and b is treated as a constant irrespective of the system. The parameters used for the specific solutions studied are given in Table 6 and a graphical representation of Eq. 22 for LiCl and KF are provided in Figure 11.

In Figure 12, the mean ionic activity and osmotic coefficient of LiCl and KF both with and without considering ion association are presented. From Figure 12a, it can be seen that the inclusion of ion-association enables the theory to provide a better theoretical representation of the mean ionic activity data by reducing the mean ionic activity coefficient. In Figure 12b, prediction of the osmotic coefficient is reported. For LiCl, the inclusion of ion association into the model reduces the osmotic coefficient bringing it into closer agreement with the experimental data at higher concentrations ($> 6 m$). For KF, although the theory with ion association provides an improved prediction of the osmotic coefficient, the trend in the experimental data is still not correctly captured.

While the inclusion of ion association improves the theoretical treatment of LiCl and KF, for salts such as NaI and LiBr, no improvement is seen even for the correlated mean ionic activity coefficient data, as the inclusion of ion-association decreases the mean ionic activity coefficient of the solution (as the ions form ion pairs the number of free ions decreases and the mean ionic activity coefficient decreases). Hence, inclusion of ion association only works in cases where the mean ionic activity coefficient is overestimated by the completely dissociated model. For NaI and LiBr, the completely dissociated SAFT-VR+DE model already underestimates the mean ionic activity coefficient at higher concentrations and so

Table 6. Salt-Specific Dispersion Energy Parameters Between the Anion and Solvent ($\epsilon_{\text{cation-H}_2\text{O}}$) and Dispersive Ion Association Energy Parameter (b) Obtained from the Correlation of Mean Ionic Activity Coefficient Data^{109,110} (γ_{\pm}) at Molality Range $> 6 m$ Using the SAFT-VR+DE Equation of State

	$\epsilon_{\text{cation-H}_2\text{O}}/k_b$ (K)	b/k_b (K)	a/k_b (K)	K^{HB} (nm^3)
LiCl	–	1.0	6797.672	1.5×10^{-3}
KF	–	1.0	7549.883	1.5×10^{-3}
LiBr	1182.599	–	–	–
NaI	399.581	–	–	–

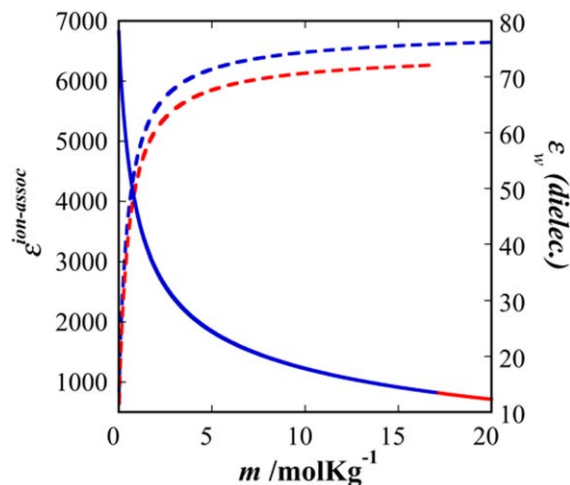


Figure 11. Association energy (dotted line) and dielectric decay (solid line) as a function of ionic concentration for LiCl (blue) and KF (red).

[Color figure can be viewed in the online issue, which is available at wileyonlinelibrary.com.]

no further improvement can be achieved by with the inclusion of ion association. However, we would not expect NaI and LiBr to form ion pairs and so this behavior is consistent with the observations of others. For example, as discussed previously studies in the literature report that ions with symmetrical sizes more readily form ion pairs compared to ions of asymmetrical sizes.⁸¹ Therefore, we would expect NaI and LiBr, which are more asymmetric in size than LiCl or KF to not significantly associate but increase their interaction with water molecules. Although, the SAFT-VR+DE approach describes the cation-solvent dispersion interaction and so would be expected to capture this behavior, anion-solvent interactions have been neglected. The need to include anion-water dispersion interactions is further supported by recent molecular dynamics simulations that investigated the effects of ion pairing in bulk water and showed that LiCl forms ion-pairs while LiBr remains completely dissociated at higher concentrations ($\sim 12 m$) with the Br ion strongly interacting with the water molecules.¹²³ Hence anion-water interactions are more significant when dealing with higher ionic concentration regimes and should not be ignored in any theoretical treatment. In the SAFT-VR+DE approach, the anion-solvent dispersive interaction parameter was initially not considered as it was found at lower concentrations ($>6 m$) to not have a significant effect on the correlated results and enabled the number of fitted parameters to be reduced. Since at higher concentrations, anion-solvent interactions appear to be significant, for NaI and LiBr anion-solvent cross-dispersive interaction parameters have been determined by fitting to the mean ionic activity coefficient data at higher molalities ($>6 m$) while keeping all other parameters unchanged. The dispersive SW interaction range (λ) is again set to 1.2 and the Lorentz–Bethelot combining rule is used to obtain the cross-interaction range parameters between the anions and solvent molecules. Since we need to parameterize the anion-solvent dispersive interaction parameter, the appropriate choice of ionic radii was also considered. As discussed previously, at lower concentrations ionic radii for several ions (Li^+ , Na^+ , F^-) were fitted and effective radii obtained in order to enable the theory to capture the structure making effect of the ionic interaction with water;

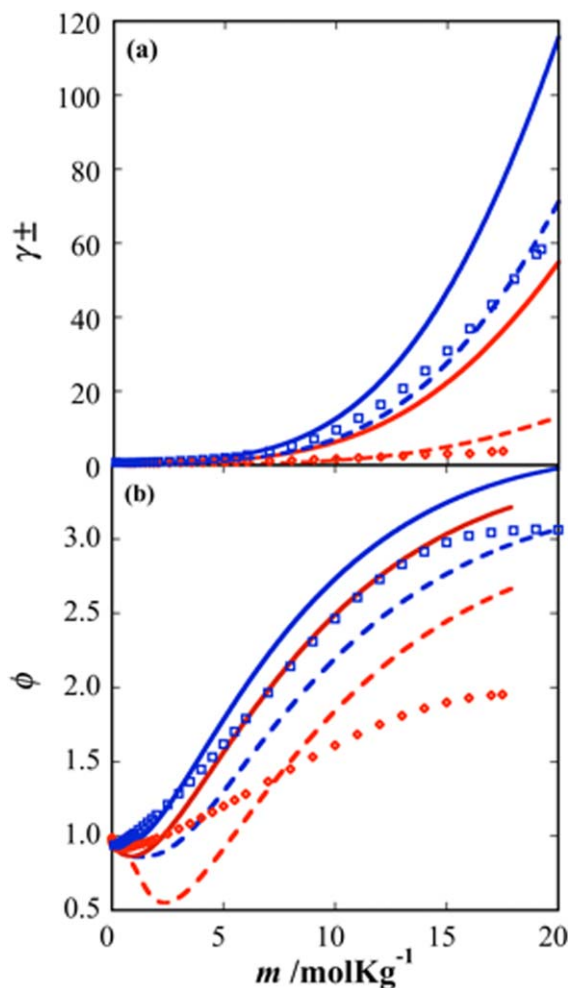


Figure 12. Comparison of the (a) mean ionic activity coefficient and (b) osmotic coefficient for LiCl (blue \square) and KF (red \diamond) from the SAFT-VR+DE equation of state without ion association (solid lines) and with ion association (dashed lines) as compared to experimental data (symbols).¹¹⁰

[Color figure can be viewed in the online issue, which is available at wileyonlinelibrary.com.]

however, at higher ionic concentrations for dissociated salts, the ion-water interactions will not impact multiple water shells due to the more concentrated salt solution and lack of free water molecules. Therefore, in this scenario, the Shannon effective ionic radii is used for Li^+ (0.076 nm) and Na^+ (0.102 nm), rather than the previously obtained fitted one. The new parameters determined for NaI and LiBr are reported in Table 6, with the other parameters remaining unchanged.

As can be seen from Figure 13, inclusion of the anion-solvent dispersive energy significantly improves the theoretical representation for LiBr and NaI. For, both LiBr and NaI the theory provides an accurate description of the mean ionic activity coefficient at higher salt concentrations. Overall, we can conclude that ion association phenomenon is salt dependent and, therefore, the addition of ion association and anion-solvent dispersion terms will be beneficial for only some systems. For the salts studied herein, the description of LiCl and KF is improved through the incorporation of ion association in to the model but for NaI and LiBr the inclusion of

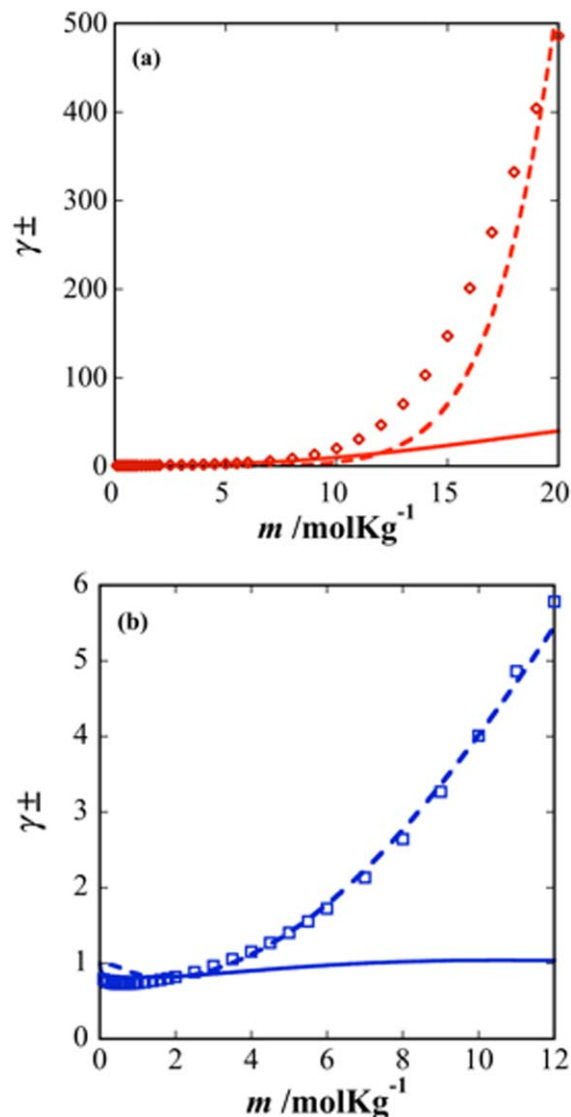


Figure 13. Comparison of the mean ionic activity coefficient for (a) LiBr (red \diamond) and (b) NaI (blue \square) obtained from the SAFT-VR+DE equation of state with (dashed lines) and without (solid line) an anion-water interaction with experimental data.

Symbols represent the experimental data.¹¹⁰ [Color figure can be viewed in the online issue, which is available at wileyonlinelibrary.com.]

anion-solvent dispersive interactions are the key to a better theoretical description. Typically, salts containing symmetric-sized ions will be more inclined to form ion-pairs at high ionic concentrations as compared to a salt formed from asymmetric ions where anion solvent interactions will be more significant.

Conclusion

In this work, we have applied the SAFT-VR+DE equations of state developed in earlier work to study 19 different 1:1 electrolyte solutions. A comprehensive study that evaluates a range of thermodynamic properties including the mean ionic activity coefficient, osmotic coefficient, water activity coefficient, density, Gibbs free energy of hydration, and the dielec-

Table 7. Summary of the Proposed Modeling Approaches Considered in This Work and the Required Adjustable Parameters for Each

Electrolytes	Molality Range (m)	Model	Adjustable Parameters
All	0–6	Fully dissociated	$\epsilon_{\text{cation-H}_2\text{O}}$ for all electrolytes, σ_{ion} for Li, Na and F ions
LiCl, KF	>6	partially associated	ϵ^{HB} , $\epsilon_{\text{cation-H}_2\text{O}}$ ^a
NaI, LiBr	>6	dissociated	$\epsilon_{\text{cation-H}_2\text{O}}$

^aParameters for all electrolytes same as for 0–6 m range.

tric decay, has been performed. For electrolyte solutions in the concentration range up to 6 m , a fully dissociated model is considered that uses a salt-specific cation-solvent dispersive energy parameter fitted to mean ionic activity coefficient data. For some systems (salts of Li, Na, and F), the ionic radii are also fitted. In comparison to other SAFT-based approaches, the use of the full non-primitive model in the SAFT-VR+DE equation of state enables improved predictions for the Gibbs free energy of hydration, especially for cations, and the prediction of the dielectric decrement with increasing ionic concentration. The results for the dielectric decay for different electrolyte solutions are qualitatively consistent with experimental observations but deviate quantitatively. We also, report the effect of temperature on thermodynamic properties such as solution densities, mean ionic activity coefficients, and osmotic coefficients for K and Na halide salts. Although the theory provides quantitatively accurate predictions of the solution densities over a range of temperatures (298.15–473.15 K), the mean ionic activities and osmotic coefficients are only in qualitative agreement. The underprediction of the dielectric constant at higher temperatures and pressures, has been identified as the key reason behind the divergence of the SAFT-V+DE predictions from the experimental data. At higher ionic concentrations (>6 m), the theory has been extended to include ion association and shown to improve the correlation and prediction of the thermodynamic properties of LiCl and KF salts. For LiBr and NaI, due to the higher asymmetry between the ions, instead of ion association, consideration of anion-solvent (water) dispersion interactions is found to improve the theoretical description of the mean ionic activity coefficient. The results demonstrate that when developing a predictive equation of state for a family of electrolyte solutions, a uniform model is not appropriate and the nature of the salt and the concentration range being studied should be taken into account and the model tailored to capture the correct interactions, as summarized in Table 7. Specifically, when studying electrolyte solutions from infinite dilution to the fused salt limit, while a fully dissociated model of electrolytes can be expected to capture the thermodynamic behavior at low to moderate concentrations at higher concentrations, with the changes in intermolecular/ionic interactions, the underlying theoretical considerations should also change. Depending upon the nature of the ions, ion association or enhanced anion-solvent interactions should be considered.

Acknowledgment

The authors gratefully acknowledge financial support from the National Science Foundation under Grant CBET-

1067642 and the U.S. Department of Energy (DOE), Office of Basic Energy Sciences, Geoscience Research Program, through Grant No. ERKCC72 of Oak Ridge National Laboratory, which is managed for DOE by UT Battelle, LLC under Contract No. DE-AC05-00OR22725.

Literature Cited

1. Enick R, Klara S. Effects of CO₂ solubility in brine on the compositional simulation of CO₂ floods. *SPE Reserv Eng*. 1992;7(2):253–258.
2. Davies RH. *Chemical Thermodynamics in Industry: Models and Computation*. Oxford: Blackwell Scientific Publishers, 1985.
3. Scrivner NC. Some Problems in Electrolyte Solutions. In: *The American Institute of Chemical Engineers Annual Meeting*. San Francisco, CA, 1984.
4. Zemaitis JF Jr, Clark DM, Rafal M, Scrivner NC. *Handbook of Aqueous Electrolyte Thermodynamics*. New York: Design Institute for Physical Property Data, American Institute of Chemical Engineers, 1986.
5. Anderko A, Wang PM, Rafal M. Electrolyte solutions: from thermodynamic and transport property models to the simulation of industrial processes. *Fluid Phase Equilib*. 2002;194:123–142.
6. Kontogeorgis GM, Folas GK. *Thermodynamic Models for Industrial Applications: From Classical and Advanced Mixing Rules to Association Theories*. John Wiley & Sons, 2010:461–523.
7. Pitzer KS. Thermodynamics of electrolytes. I. Theoretical basis and general equations. *J Phys Chem*. 1973;77(2):268–277.
8. Loehe JR, Donohue MD. Recent advances in modeling thermodynamic properties of aqueous strong electrolyte systems. *AIChE J*. 1997;43(1):180–195.
9. Pitzer KS, Mayorga G. Thermodynamics of electrolytes 2. Activity and osmotic coefficients for strong electrolytes with one or both ions univalent. *J Phys Chem*. 1973;77(19):2300–2308.
10. Pitzer KS, Mayorga G. Thermodynamics of electrolytes. III. Activity and osmotic coefficients for 2-2 electrolytes. *J Solution Chem*. 1974;3(7):539–546.
11. Chen C-C, Britt HI, Boston JF, Evans LB. Local composition model for excess Gibbs energy of electrolyte systems. Part I: single solvent, single completely dissociated electrolyte systems. *AIChE J*. 1982;28(4):588–596.
12. Robinson RA, Wood RH, Reilly PJ. Calculation of excess Gibbs energies and activity coefficients from isopiestic measurements on mixtures of lithium and sodium salts. *J Chem Thermodyn*. 1971;3(4):461–471.
13. Reilly PJ, Wood RH. Prediction of the properties of mixed electrolytes from measurements on common ion mixtures. *J Phys Chem*. 1969;73(12):4292–4297.
14. Scatchard G, Rush RM, Johnson JS. Osmotic and activity coefficients for binary mixtures of sodium chloride, sodium sulfate, magnesium sulfate, and magnesium chloride in water at 25 degrees 3. Treatment with ions as components. *J Phys Chem*. 1970;74(21):3786.
15. Pitzer KS, Roy RN, Silvester LF. Thermodynamics of electrolytes 7. Sulfuric-acid. *J Am Chem Soc*. 1977;99(15):4930–4936.
16. Pitzer KS. Ionic fluids. *J Phys Chem*. 1984;88(13):2689–2697.
17. Pitzer KS. Thermodynamics of unsymmetrical electrolyte mixtures - enthalpy and heat-capacity. *J Phys Chem*. 1983;87(13):2360–2364.
18. Meissner HP, Kusik CL. Activity-coefficients of strong electrolytes in multicomponent aqueous-solutions. *AIChE J*. 1972;18(2):294–298.
19. Meissner HP, Tester JW, Kusik CL. Activity-coefficients of strong electrolytes in aqueous-solution - effect of temperature. *AIChE J*. 1972;18(3):661–662.
20. Cruz JL, Renon H. New thermodynamic representation of binary electrolyte-solutions non-ideality in whole range of concentrations. *AIChE J*. 1978;24(5):817–830.
21. Liu Y, Harvey AH, Prausnitz JM. Thermodynamics of concentrated electrolyte-solutions. *Chem Eng Commun*. 1989;77:43–66.
22. Friedman HL. Electrolyte solutions at equilibrium. *Annu Rev Phys Chem*. 1981;32(1):179–204.
23. Pitzer KS, Schreiber DR. The restricted primitive model for ionic fluids - properties of the vapor and the critical region. *Mol Phys*. 1987;60(5):1067–1078.
24. Stell G, Lebowitz JL. Equilibrium properties of a system of charged particles. *J Chem Phys*. 1968;49:3706–3717.
25. Henderson D. Perturbation theory, ionic fluids, and the electric double layer. *ACS Symp Ser*. 1983;204:47–71.
26. Henderson D, Blum L, Tani A. Equation of state of ionic fluids. *ACS Symp Ser*. 1986;300:281–296.
27. Jin G, Donohue MD. An equation of state for electrolyte-solutions. 1. Aqueous systems containing strong electrolytes. *Ind Eng Chem Res*. 1988;27(6):1073–1084.
28. Jin G, Donohue MD. An equation of state for electrolyte-solutions. 2. Single volatile weak electrolytes in water. *Ind Eng Chem Res*. 1988;27(9):1737–1743.
29. Jin G, Donohue MD. An equation of state for electrolyte-solutions. 3. Aqueous-solutions containing multiple salts. *Ind Eng Chem Res*. 1991;30(1):240–248.
30. Vimalchand P, Celmins I, Donohue MD. VLE calculations for mixtures containing multipolar compounds using the perturbed anisotropic chain theory. *AIChE J*. 1986;32(10):1735–1738.
31. Percus J, Yevick G. Hard-core insertion in the many-body problem. *Phys Rev*. 1964;136(1B):B290.
32. Lebowitz J, Percus J. Mean spherical model for lattice gases with extended hard cores and continuum fluids. *Phys Rev*. 1966;144(1):251.
33. Waisman E, Lebowitz JL. Mean spherical model integral equation for charged hard spheres I. Method of solution. *J Chem Phys*. 1972;56:3086.
34. Waisman E. The radial distribution function for a fluid of hard spheres at high densities: mean spherical integral equation approach. *Mol Phys*. 1973;25(1):45–48.
35. Wertheim M. Exact solution of the mean spherical model for fluids of hard spheres with permanent electric dipole moments. *J Chem Phys*. 1971;55:4291.
36. Palmer R, Weeks J. Exact solution of the mean spherical model for charged hard spheres in a uniform neutralizing background. *J Chem Phys*. 1973;58:4171.
37. Adelman S, Deutch J. Exact solution of the mean spherical model for simple polar mixtures. *J Chem Phys*. 1973;59:3971.
38. Adelman S, Deutch J. Exact solution of the mean spherical model for strong electrolytes in polar solvents. *J Chem Phys*. 1974;60:3935.
39. Blum L. Solution of the mean spherical approximation for hard ions and dipoles of arbitrary size. *J Stat Phys*. 1978;18(5):451–474.
40. Blum L, Wei D. Analytical solution of the mean spherical approximation for an arbitrary mixture of ions in a dipolar solvent. *J Chem Phys*. 1987;87:555.
41. Golovko M, Protsykevich I. Analytic solution of the mean spherical approximation for ion-dipole model in a neutralizing background. *J Stat Phys*. 1989;54(3–4):707–733.
42. Blum L. Mean spherical model for asymmetric electrolytes: I. Method of solution. *Mol Phys*. 1975;30(5):1529–1535.
43. Blum L. Mean spherical model for a mixture of charged spheres and hard dipoles. *Chem Phys Lett*. 1974;26(2):200–202.
44. Hoye JS, Stell G. Ionic solution in a molecular polar-solvent. *J Chem Phys*. 1978;68(9):4145–4150.
45. McCabe C, Galindo A. SAFT associating fluids and fluid mixtures. In: Goodwin AR, Sengers J, Peters CJ, editors. *Applied Thermodynamics of Fluids*. 2010:215–279. DOI:10.1039/9781849730983.
46. Zhao H, dos Ramos MC, McCabe C. Development of an equation of state for electrolyte solutions by combining the statistical associating fluid theory and the mean spherical approximation for the nonprimitive model. *J Chem Phys*. 2007;126:244503.
47. Chapman WG, Jackson G, Gubbins KE. Phase equilibria of associating fluids: chain molecules with multiple bonding sites. *Mol Phys*. 1988;65(5):1057–1079.
48. Chapman WG, Gubbins KE, Jackson G, Radosz M. SAFT: equation-of-state solution model for associating fluids. *Fluid Phase Equilib*. 1989;52:31–38.
49. Chapman WG, Gubbins KE, Jackson G, Radosz M. New reference equation of state for associating liquids. *Ind Eng Chem Res*. 1990;29(8):1709–1721.
50. Wertheim M. Fluids with highly directional attractive forces. II. Thermodynamic perturbation theory and integral equations. *J Stat Phys*. 1984;35(1–2):35–47.
51. Wertheim M. Fluids with highly directional attractive forces. I. Statistical thermodynamics. *J Stat Phys*. 1984;35(1–2):19–34.
52. Wertheim M. Fluids with highly directional attractive forces. IV. Equilibrium polymerization. *Journal of Stat Phys*. 1986;42(3–4):477–492.
53. Wertheim M. Fluids with highly directional attractive forces. III. Multiple attraction sites. *J Stat Phys*. 1986;42(3–4):459–476.
54. Muller EA, Gubbins KE. Molecular-based equations of state for associating fluids: a review of SAFT and related approaches. *Ind Eng Chem Res*. 2001;40(10):2193–2211.

55. Economou IG. Statistical associating fluid theory: a successful model for the calculation of thermodynamic and phase equilibrium properties of complex fluid mixtures. *Ind Eng Chem Res.* 2002;41(5):953–962.
56. Tan SP, Adidharma H, Radosz M. Recent advances and applications of statistical associating fluid theory. *Ind Eng Chem Res.* 2008;47(21):8063–8082.
57. Galindo A, Gil-Villegas A, Jackson G, Burgess AN. SAFT-VRE: phase behavior of electrolyte solutions with the statistical associating fluid theory for potentials of variable range. *J Phys Chem B.* 1999;103(46):10272–10281.
58. Tan SP, Adidharma H, Radosz M. Statistical associating fluid theory coupled with restricted primitive model to represent aqueous strong electrolytes. *Ind Eng Chem Res.* 2005;44(12):4442–4452.
59. Behzadi B, Patel B, Galindo A, Ghotbi C. Modeling electrolyte solutions with the SAFT-VR equation using Yukawa potentials and the mean-spherical approximation. *Fluid Phase Equilib.* 2005; 236(1):241–255.
60. Schreckenber JMA, Dufal S, Haslam AJ, Adjiman CS, Jackson G, Galindo A. Modelling of the thermodynamic and solvation properties of electrolyte solutions with the statistical associating fluid theory for potentials of variable range. *Mol Phys.* 2014;112(17): 2339–2364.
61. Uematsu M, Franck EU. Static dielectric-constant of water and steam. *J Phys Chem Ref Data.* 1980;9(4):1291–1306.
62. Hudson GH, McCoubrey JC. Intermolecular forces between unlike molecules. A more complete form of the combining rules. *Trans Faraday Soc.* 1960;56:761–766.
63. Ji XY, Tan SP, Adidharma H, Radosz M. Statistical associating fluid theory coupled with restricted primitive model to represent aqueous strong electrolytes: multiple-salt solutions. *Ind Eng Chem Res.* 2005;44(19):7584–7590.
64. Ji XY, Tan SP, Adidharma H, Radosz M. Statistical associating fluid theory coupled with restrictive primitive model extended to bivalent ions. SAFT2: 2. Brine/seawater properties predicted. *J Phys Chem B.* 2006;110(33):16700–16706.
65. Blum L, Høye JS. Mean spherical model for asymmetric electrolytes. 2. Thermodynamic properties and pair correlation-function. *J Phys Chem.* 1977;81(13):1311–1317.
66. Cameretti LF, Sadowski G, Møllerup JM. Modeling of aqueous electrolyte solutions with perturbed-chain statistical associated fluid theory. *Ind Eng Chem Res.* 2005;44(9):3355–3362.
67. Held C, Cameretti LF, Sadowski G. Modeling aqueous electrolyte solutions: part 1. Fully dissociated electrolytes. *Fluid Phase Equilib.* 2008;270(1):87–96.
68. Held C, Sadowski G. Modeling aqueous electrolyte solutions. Part 2. Weak electrolytes. *Fluid Phase Equilib.* 2009;279(2): 141–148.
69. Held C, Prinz A, Wallmeyer V, Sadowski G. Measuring and modeling alcohol/salt systems. *Chem Eng Sci.* 2012;68(1):328–339.
70. Liu WB, Li YG, Lu JF. A new equation of state for real aqueous ionic fluids based on electrolyte perturbation theory, mean spherical approximation and statistical associating fluid theory. *Fluid Phase Equilib.* 1999;158:595–606.
71. Cotterman RL, Schwarz BJ, Prausnitz JM. Molecular thermodynamics for fluids at low and high-densities. 1. Pure fluids containing small or large molecules. *AIChE J.* 1986;32(11):1787–1798.
72. Mavroyannis C, Stephen MJ. Dispersion forces. *Mol Phys.* 1962; 5(6):629–638.
73. Liu Z, Wang W, Li Y. An equation of state for electrolyte solutions by a combination of low-density expansion of non-primitive mean spherical approximation and statistical associating fluid theory. *Fluid Phase Equilib.* 2005;227(2):147–156.
74. Liu ZP, Li YG, Lu JF. Low-density expansion of the solution of mean spherical approximation for ion-dipole mixtures. *J Phys Chem B.* 2002;106(20):5266–5274.
75. Myers JA, Sandler SI, Wood RH. An equation of state for electrolyte solutions covering wide ranges of temperature, pressure, and composition. *Ind Eng Chem Res.* 2002;41(13):3282–3297.
76. Furst W, Renon H. Representation of excess properties of electrolyte-solutions using a new equation of state. *AIChE J.* 1993; 39(2):335–343.
77. Rozmus J, de Hemptinne JC, Galindo A, Dufal S, Mougin P. Modeling of strong electrolytes with ePPC-SAFT up to high temperatures. *Ind Eng Chem Res.* 2013;52(29):9979–9994.
78. Schmidt E, Grigull U. *Properties of Water and Steam in SI-Units.* New York: Springer Verlag, 1982.
79. Herzog S, Gross J, Arlt W. Equation of state for aqueous electrolyte systems based on the semirestricted non-primitive mean spherical approximation. *Fluid Phase Equilib.* 2010;297(1):23–33.
80. Fedotova MV, Kruchinin SE, Rahman HMA, Buchner R. Features of ion hydration and association in aqueous rubidium fluoride solutions at ambient conditions. *J Mol Liq.* 2011;159(1):9–17.
81. Fennell CJ, Bizjak A, Vlachy V, Dill KA. Ion pairing in molecular simulations of aqueous alkali halide solutions. *J Phys Chem B* 2009;113(19):6782–6791.
82. Driesner T, Seward TM, Tironi IG. Molecular dynamics simulation study of ionic hydration and ion association in dilute and 1 molal aqueous sodium chloride solutions from ambient to supercritical conditions. *Geochim Cosmochim Acta.* 1998;62(18):3095–3107.
83. GilVillegas A, Galindo A, Whitehead PJ, Mills SJ, Jackson G, Burgess AN. Statistical associating fluid theory for chain molecules with attractive potentials of variable range. *J Chem Phys.* 1997; 106(10):4168–4186.
84. Wei D, Blum L. The mean spherical approximation for an arbitrary mixture of ions in a dipolar solvent: approximate solution, pair correlation functions, and thermodynamics. *J Chem Phys.* 1987;87: 2999.
85. Zhao H, Ding Y, McCabe C. Phase behavior of dipolar associating fluids from the SAFT-VR+D equation of state. *J Chem Phys.* 2007;127(8):084514.
86. Clough SA, Beers Y, Klein GP, Rothman LS. Dipole-moment of water from Stark measurements of H₂O, HDO, and D₂O. *J Chem Phys.* 1973;59(5):2254–2259.
87. Coulson CA, Eisenber D. Interactions of H₂O molecules in ice. 2. Interaction energies of H₂O molecules in ice. *Proc R Soc London Ser A Math Phys Sci.* 1966;291(1427):454–459.
88. Silvestrelli PL, Parrinello M. Water molecule dipole in the gas and in the liquid phase. *Phys Rev Lett.* 1999;82(16):3308–3311.
89. Rappoport Z. *CRC Handbook of Tables for Organic Compound Identification, 3rd ed.* Boca Raton, FL: CRC Press, 1967:563p.
90. McCabe C, Kiselev SB. A crossover SAFT-VR equation of state for pure fluids: preliminary results for light hydrocarbons. *Fluid Phase Equilib.* 2004;219(1):3–9.
91. Lafitte T, Bessieres D, Pineiro MM, Daridon JL. Simultaneous estimation of phase behavior and second-derivative properties using the statistical associating fluid theory with variable range approach. *J Chem Phys.* 2006;124(2):024509.
92. Kirkpatrick S, Gelatt CD, Vecchi MP. Optimization by simulated annealing. *Science.* 1983;220(4598):671–680.
93. Dolan WB, Cummings PT, Levan MD. Process optimization via simulated annealing - application to network design. *AIChE J.* 1989;35(5):725–736.
94. Albright PC, Sengers JV, Nicoll JF, Leykoo M. A crossover description for the thermodynamic properties of fluids in the critical region. *Int J Thermophys.* 1986;7(1):75–85.
95. McCabe C, Kiselev SB. Application of crossover theory to the SAFT-VR equation of state: SAFT-VRX for pure fluids. *Ind Eng Chem Res.* 2004;43(11):2839–2851.
96. Adidharma H, Radosz M. Prototype of an engineering equation of state for heterosegmented polymers. *Ind Eng Chem Res.* 1998; 37(11):4453–4462.
97. Shannon RD. Revised effective ionic-radii and systematic studies of interatomic distances in halides and chalcogenides. *Acta Crystallogr A.* 1976;32(5):751–767.
98. Goldschmidt VM. Kristallbau und Chemische Zusammensetzung. *Berichte der Deutschen Chemischen Gesellschaft, Math Nat k1.* 1927;60(2):1263–1296.
99. Pauling L. The nature of the chemical bond—1992. *J Chem Educ.* 1992;69(7):519.
100. Shannon RD, Prewitt CT. Revised values of effective ionic radii. *Acta Crystallogr B.* 1970;B26:1046–1048.
101. Gourary BS, Adrian FJ. Wave functions for electron-excess color centers in alkali halide crystals. *Solid State Phys.* 1960;10:127–247.
102. Levy HA, Danford MD. Diffraction studies of the structure of molten salts. *Molten Salt Chemistry.* New York: Interscience Publishers, 1964.
103. Mahler J, Persson I. A study of the hydration of the alkali metal ions in aqueous solution. *Inorg Chem.* 2012;51(1):425–438.
104. Bergstrom PA, Lindgren J, Kristiansson O. An Ir study of the hydration of ClO₄⁻, NO₃⁻, I⁻, Br⁻, Cl⁻, and SO₄²⁻ anions in aqueous-solution. *J Phys Chem.* 1991;95(22):8575–8580.
105. Levenberg K. A method for the solution of certain non-linear problems in least squares. *Q Appl Math.* 1944;2:164–168.

106. Dufal S. Ph.D. Thesis. Development and application of advanced thermodynamic molecular description for complex reservoir fluids containing carbon dioxide and brines, Imperial College London, UK, 2013.
107. Pye CC, Rudolph W, Poirier RA. An ab initio investigation of lithium ion hydration. *J Phys Chem.* 1996;100(2):601–605.
108. Abraham MH, Liszi J, Papp E. Calculations on ionic solvation. Part 6. *J Chem Soc Faraday Trans 1.* 1982;78(1):197–211.
109. Robinson RA, Stokes RH. *Electrolyte Solutions: The Measurement and Interpretation of Conductance, Chemical Potential, and Diffusion in Solutions of Simple Electrolytes, 2nd ed.* London: Butterworths, 1959: xv, 571 p.
110. Hamer WJ, Wu Y-C. Osmotic coefficient and mean activity coefficient of uni-univalent electrolytes in water at 25 C. *J Phys Ref Data.* 1972;1(4):1047–1100.
111. Eiberweiser A, Buchner R. Ion-pair or ion-cloud relaxation? On the origin of small-amplitude low-frequency relaxations of weakly associating aqueous electrolytes. *J Mol Liq.* 2012;176:52–59.
112. Gil-Villegas A, Galindo A, Jackson G. A statistical associating fluid theory for electrolyte solutions (SAFT-VRE). *Mol Phys.* 2001; 99(6):531–546.
113. Paunovic M, Schlesinger M. *Fundamentals of Electrochemical Deposition, 2nd ed.* Hoboken, NJ: Wiley-Interscience, 2006: x, 373 p.
114. Debye PJW. *Polar Molecules.* New York: Chemical Catalog Company, Inc., 1929:172 p.
115. Wei YZ, Chiang P, Sridhar S. Ion size effects on the dynamic and static dielectric-properties of aqueous alkali solutions. *J Chem Phys.* 1992;96(6):4569–4573.
116. Wei YZ, Sridhar S. Dielectric-spectroscopy up to 20 Ghz of LiCl/H₂O solutions. *J Chem Phys.* 1990;92(2):923–928.
117. Hasted JB, Ritson DM, Collie CH. Dielectric properties of aqueous ionic solutions. Parts I and II. *J Chem Phys.* 1948;16:1–21.
118. Maribo-Mogensen B, Kontogeorgis GM, Thomsen K. Modeling of dielectric properties of aqueous salt solutions with an equation of state. *J Phys Chem B.* 2013;117(36):10523–10533.
119. Archer DG. Thermodynamic properties of the NaCl+H₂O system. 2. Thermodynamic properties of NaCl(Aq), NaCl.2H₂O(Cr), and phase-equilibria. *J Phys Chem Ref Data.* 1992;21(4):793–829.
120. Panichajakul CC, Woolley EM. *Thermodynamic Behavior of Electrolytes in Mixed Solvents*, Vol. 155. Washington, DC: American Chemical Society, 1976.
121. Sen B, Roy RN, Gibbons JJ, Johnson DA, Adcock LH. *Thermodynamic Behavior of Electrolytes in Mixed Solvents II*, Vol. 177. Washington, DC: American Chemical Society, 1979.
122. Fuoss RM. Conductimetric determination of thermodynamic pairing constants for symmetrical electrolytes. *Proc Natl Acad Sci USA.* 1980;77(1):34–38.
123. Niazi A, Olszowy N, Rabideau BD, Ismail AE. Measurement of enthalpy and free energy changes for dissolution in concentrated electrolyte media using molecular simulations. In: *AICHE Annual Conference*, Atlanta, GA, 2014.

Appendix A

The objective function ($\text{obj}(P, \rho_{\text{liq}})$) used to obtain the SAFT-VR+D parameters for water is given by

$$\text{obj}(P, \rho_{\text{liq}}) = \frac{1}{N_{\text{pt}}} \sum_{i=1}^{N_{\text{pt}}} \left\{ \left| \frac{P_i^{\text{theo}} - P_i^{\text{exp}}}{P_i^{\text{exp}}} \right| + \left| \frac{\rho_i^{\text{theo}} - \rho_i^{\text{exp}}}{\rho_i^{\text{exp}}} \right| \right\} \times 100\% \quad (\text{A1.1})$$

where N_{pt} is the number of experimental points being evaluated, P_i^{exp} and P_i^{theo} are the experimental and calculated pressure; ρ_i^{exp} and ρ_i^{theo} are the experimental and calculated saturated liquid density, respectively.

The SAFT-VR+DE parameters for aqueous electrolyte solutions were obtained by optimizing the following objective function

$$\text{obj}(\gamma_{\pm}) = \frac{1}{N_{\text{pt}}} \sum_{i=1}^{N_{\text{pt}}} \left| \frac{\gamma_{\pm i}^{\text{theo}} - \gamma_{\pm i}^{\text{exp}}}{\gamma_{\pm i}^{\text{exp}}} \right| \times 100\% \quad (\text{A1.2})$$

where N_{exp} is the number of experimental data points and γ_{\pm} the mean ionic activity coefficient. In Table A1, the correlated %AAD for the mean ionic activity coefficients are reported using ionic radii proposed by Mähler and Persson¹⁰³ for Li⁺, Na⁺, and F⁻.

In Table A2, the %AAD of the SAFT-VR+DE theoretical predictions from the experimental data is reported for the osmotic coefficient (Φ), aqueous activity coefficient (γ_w) and density (ρ). The AADs in thermodynamic properties is expressed using AAD M (%)

Table A1. %AAD in γ_{\pm} for Salts Containing Li⁺, Na⁺, F⁻ Using Ionic Radii Proposed by Mähler et al.

Salt	% AAD γ_{\pm}	Molality
LiCl	33.65	0.1–6.0
LiBr	29.08	0.1–6.0
LiI	23.84	0.1–3.0
NaF	4.93	0.1–1.0
NaCl	20.94	0.1–6.0
NaBr	8.80	0.1–4.0
NaI	12.99	0.1–3.5
KF	13.64	0.1–4.0
RbF	15.25	0.1–3.5
CsF	6.96	0.1–3.5

Table A2. Comparison Between Experimental^{109,110} and SAFT-VR+DE equation of State Predictions for Osmotic Coefficient (Φ), Water Activity Coefficient (γ_w), and Solution Densities (ρ) for Different Electrolytes

Salts	%AAD Φ	% AAD γ_w	%AAD ρ	Molality
LiCl	4.92	6.72	2.66	0.1–6.0
LiBr	2.53	7.50	3.19	0.1–6.0
LiI	4.64	4.11	2.83	0.1–3.0
NaF	0.57	1.99	NA	0.1–1.0
NaCl	5.58	6.81	1.09	0.1–6.0
NaBr	1.53	5.05	2.16	0.1–4.0
NaI	4.79	4.70	2.09	0.1–3.5
KF	5.84	4.80	2.80	0.1–4.0
KCl	3.79	5.41	1.74	0.1–4.5
KBr	2.02	6.74	1.77	0.1–5.5
KI	4.90	5.88	2.61	0.1–4.5
RbF	3.69	4.43	2.77	0.1–3.5
RbCl	1.85	6.25	3.71	0.1–5.0
RbBr	3.36	6.47	NA	0.1–5.0
RbI	7.13	6.82	2.57	0.1–5.0
CsF	1.34	4.49	4.50	0.1–3.5
CsCl	3.73	7.86	3.05	0.1–6.0
CsBr	5.63	6.69	2.47	0.1–5.0
CsI	5.72	4.29	3.03	0.1–3.0

Table A3. Comparison Between Experimental and SAFT-VRE Theoretical Predictions for the Gibbs Free Energy of Solvation for Different Aqueous Electrolytes

Salt	ΔG^{hyd} (KJ/mol)	ΔG^{hyd} Expt. (KJ/mol)
LiCl	29.85	–833.4
LiBr	51.88	–807.1
LiI	65.17	–772
NaCl	–21.26	–727.7
NaBr	0.77	–701.4
NaI	11.61	–666.3
KCl	59.11	–655.9
KBr	81.13	–629.6
KI	94.43	–594.5

$$\text{AADM}(\%) = \frac{1}{N_{\text{pt}}} \sum_{i=1}^{N_{\text{pt}}} \left| \frac{M^{\text{theo}} - M^{\text{exp}}}{M^{\text{exp}}} \right| \times 100\%$$

where M^{exp} and M^{theo} are the experimental and theoretically calculated thermodynamic properties [i.e., osmotic coefficient (ϕ), water activity coefficient (γ_w), and solution density (ρ)], respectively.

In Table A3, the Gibbs free energy of hydration calculated from the SAFT-VRE⁵⁷ equation of state using the RPM is reported. Parameters for this study have been taken from the original work of Galindo et al.⁵⁷

Appendix B

The free energy contribution for electrostatic interactions A^{el} is determined using the MSA for mixtures of ions and dipoles developed by Blum and Wei and Golovko.^{40,41,84} Within the MSA, the expression for the electrostatic free energy is given by

$$\frac{A^{\text{el}}}{Vk_bT} = \frac{E^{\text{el}}}{Vk_bT} - J - J' \quad (\text{B1})$$

where, V is the total volume of the solution and E^{el}/Vk_bT is an internal energy per unit of volume defined as

$$\frac{E^{\text{el}}}{Vk_bT} = \frac{1}{4\pi} \left\{ \alpha_0^2 \sum_{k=1}^2 \rho_k z_k N_k - 2\alpha_2 \alpha_0 \rho_n B^{10} - \frac{2\alpha_2^2 \rho_n b_2}{\sigma_n^3} \right\} \quad (\text{B2})$$

with terms J and J' defined⁴¹ by

$$J = \frac{1}{12\pi} \left\{ \alpha_0^2 \sum_{k=1}^2 \rho_k z_k N_k - 2\alpha_0 \alpha_2 \rho_n B^{10} - \frac{6\alpha_2^2 \rho_n b_2}{\sigma_n^3} \right\} \quad (\text{B3})$$

$$J' = \frac{\pi}{3} \sum_i \sum_j \rho_i \rho_j \sigma_{ij} \left\{ \sum_{nm} \frac{(-1)^l}{2l+1} \left[g_{ij}^{nm}(\sigma_{ij}) \right]^2 - \left[g_{ij}^{hs}(\sigma_{ij}) \right]^2 \right\} \quad (\text{B4})$$

Here, $g_{ij}^{nm}(\sigma_{ij})$ are the contact values of the RDF invariant expansion coefficients and $g_{ij}^{hs}(\sigma_{ij})$ is the hard-sphere contact value. All other terms are defined as follows^{40,84}

$$\begin{aligned} \alpha_0^2 &= \frac{4\pi^2}{k_bT}, & \alpha_2^2 &= \frac{4\pi\mu^2}{3k_bT} \\ \beta_3 &= 1 + \frac{b_2}{3}, & \beta_6 &= 1 - \frac{b_2}{6} \\ \lambda &= \frac{\beta_3}{\beta_6}, & y_1 &= \frac{4}{\beta_6(1+\lambda)^2} \\ \Delta\Gamma_i &= \frac{V\eta\rho_n\sigma_n^2\sigma_i^2B^{10}}{8\beta_6(\sigma_n+\lambda\sigma_i)} \end{aligned} \quad (\text{B5})$$

$$D_i^F = \frac{z_i\beta_6}{2(1+\sigma_i\Gamma-\Delta\Gamma_i)}, m_i = \frac{V\eta D_i^F}{\sigma_n+\lambda\sigma_i}$$

$$D = 1 + V\eta^2\rho_n\sigma_n^2 \sum_{i=1}^{n-1} \frac{\rho_i\sigma_i^2(D_i^F)^2}{[2\beta_6(\sigma_n+\lambda\sigma_i)]^2}, D_{ac} = \sum_{i=1}^{n-1} \rho_i(D_i^F)^2$$

$$\Gamma_i^s = \frac{(1+\Gamma\sigma_i-\Delta\Gamma_i)D-1}{\sigma_i}, \Omega_{10} = V\eta \sum_{i=1}^{n-1} \frac{\rho_i\sigma_i(D_i^F)^2}{[2\beta_6(\sigma_n+\lambda\sigma_i)]^2}$$

$$N_i = \frac{2D_i^F}{\beta_6\sigma_i} \left[1 + \frac{V\eta\rho_n\sigma_n^3B^{10}\sigma_i}{24(\sigma_n+\lambda\sigma_i)} \right] - \frac{z_i}{\sigma_i}$$

$$\begin{aligned} a_i^0 &= \frac{\beta_6\Gamma_i^s D_i^F}{D_{ac}}, & a_n^1 &= \frac{D\beta_6}{2D_{ac}} \left[\frac{\sigma_n B^{10}}{2} + \frac{\Omega_{10}\lambda}{D\beta_6} \right] \\ -k_{ni}^{10} &= \frac{\sigma_n^2 D_i^F}{2D\beta_6^2} \left[\frac{V\eta}{\sigma+\lambda\sigma_i} + \frac{\Omega_{10}\Gamma_i^s}{D_{ac}} \right] + \frac{\sigma_n^3 B^{10} a_i^0}{12\beta_6} \\ 1 - \rho_n k_{nm}^{11} &= \frac{1}{D\beta_6} \left[\lambda + \frac{\rho_n \sigma_n^2 \Omega_{10} a_n^1}{2\beta_6^2} \right] + \frac{\rho_n \sigma_n^3 B^{10} a_n^1}{12\beta_6} \end{aligned}$$

where Γ , B^{10} , and b_2 are obtained numerically by solving the following equations

$$\sum_{i=1}^{n-1} \rho_i (a_i^0)^2 + \rho_n (\sigma_n^1)^2 = \alpha_0^2 \quad (\text{B6})$$

$$-\sum_{i=1}^{n-1} \rho_i a_i^0 k_{ni}^{10} + a_n^1 (1 - \rho_n k_{nm}^{11}) = \alpha_0 \alpha_2 \quad (\text{B7})$$

$$(1 - \rho_n k_{nm}^{11})^2 + \rho_n \sum_{i=1}^{n-1} \rho_i (k_{ni}^{10})^2 = y_1^2 + \rho_n \alpha_2^2 \quad (\text{B8})$$

Additionally, we should note that compared to Eq. 2.17 of Wei et al.⁸⁴, we calculate V_η from known Γ , B^{10} , and b_2 , by numerically solving the following equation

$$B^{10} = \frac{\beta_6 V_\eta}{2} \sum_{i=1}^{n-1} \frac{\rho_i z_i^2}{(\sigma_n + \sigma_i \lambda)(1 + \Gamma \sigma_i + \Delta \Gamma_i)} \quad (\text{B9})$$

where, $\Delta\Gamma_i$ is given by Eq. B5 and is proportional to V_η . Obtaining the solution in this way makes our solution of the theory numerically consistent with the SNPM solution, that is, the case of equal-size ions. Therefore, our numerical procedure consists of simultaneous solution of four Eqs. B6–B9 for four unknowns; Γ , B^{10} , b_2 , and V_η .

The contact values of the invariant expansion coefficients of the RDF in Eq. B4 is given by

$$\begin{aligned} g_{ij}^{hs}(\sigma_{ij}) &= \frac{1}{1-\zeta_3} + \frac{\pi\sigma_i\sigma_j\zeta_2}{4(1-\zeta_3)\sigma_{ij}} \\ g_{ij}^{000} \left(\sigma_{ij} = \frac{Q_{ij}^{00}}{2\pi\sigma_{ij}} \right) & \end{aligned} \quad (\text{B10})$$

$$g^{011}(\sigma_{in}) = \frac{\sqrt{3}Q_{in}^{01}}{2\pi\sigma_{in}}$$

$$g_{nm}^{110}(\sigma_{nm}) = \frac{Q_{nm}^{11} + \frac{2q'}{\rho_n\sigma_n^2}}{2\sqrt{3}\pi\sigma_n}$$

$$g_{nm}^{112}(\sigma_{nm}) = \frac{\sqrt{10} \left(Q_{nm}^{11} - \frac{q'}{\rho_n\sigma_n^2} \right)}{2\sqrt{3}\pi\sigma_n} \quad (\text{B11})$$

where

$$q' = \frac{-b_2(1-\lambda)(\lambda+3)}{(1+\lambda)^2}$$

and

$$Q_{ij}^{mn} = \left. \frac{\partial Q_{ij}^{mn}(r)}{\partial r} \right|_{r=\sigma_{ij}}$$

are the contact values of the Baxter factorization function expansion coefficients,^{40,84} and are given by

$$Q_{ij}^{00} = \frac{2\pi}{\Delta} \left(\sigma_{ij} + \frac{\pi\sigma_i\sigma_j\zeta_2}{4\Delta} \right) - \frac{1}{2} D_i^F D_j^F \left(\frac{\rho_n \sigma_n^2 v_\eta^2}{D\beta_6^2 (\sigma_n + \lambda\sigma_i)(\sigma_n + \lambda\sigma_j)} + \frac{4\Gamma_i^s \Gamma_j^s}{DD_{ac}} \right)$$

$$Q_{in}^{00} = Q_{ni}^{00} = \frac{2\pi}{\Delta} \left(\sigma_{in} + \frac{\pi\sigma_i\sigma_n\zeta_2}{4\Delta} \right)$$

$$Q_{ij}^{01} = \frac{D_i^F}{D\beta_6} \left(\frac{\lambda v_\eta}{\sigma_n + \lambda\sigma_i} + 2\Gamma_i^s a_n^1 \right)$$

$$Q_{ni}^{10} = \frac{D_i^F}{D\beta_6} \left(\frac{\lambda v_\eta}{\sigma_n + \lambda\sigma_i} + 2\Gamma_i^s a_n^1 \right)$$

$$Q_{ij}^{11} = \frac{2\lambda}{D\rho_n\sigma_n^2} \left(\lambda + \frac{\rho_n\sigma_n^2\Omega^{10}a_n^1}{2\beta_6^2} \right) + \frac{\sigma_n B^{10}a_n^1}{2\beta_6} - \frac{2}{\rho_n\sigma_n^2}$$

The ionic excess chemical potential is given by,

$$\beta\mu_i = \frac{z_i(\alpha_0^2 N_i - \alpha_0\alpha_2\rho_n m_i)}{4\pi}$$

and the chemical potential of dipolar molecules is given by,

$$\beta\mu_n = \frac{(-\alpha_0\alpha_2 B_{10} - 2\alpha_2^2 b_2/\sigma_n^3)}{4\pi}$$

Since in the MSA, the excess Gibbs free energy equals the excess internal energy, the pressure is given by

$$\beta P = \frac{\beta(E-A)}{V}$$

Manuscript received Jan. 18, 2015, and revision received Apr. 24, 2015.